

## ENCLOSURE 2

MFN 10-034

Marathon-Ultra Control Rod Assembly, NEDO-33284  
Supplement 1, Revision 0, January 2010

Non-Proprietary Information

### IMPORTANT NOTICE

Enclosure 2 is a non-proprietary version of the Marathon-Ultra Control Rod Assembly, NEDE-33284P Supplement 1, Revision 0, January 2010 from Enclosure 1, which has the proprietary information removed. Portions that have been removed are indicated by open and closed double brackets as shown here [[ ]].



**HITACHI**

GE Hitachi Nuclear Energy

NEDO-33284 Supplement 1  
Revision 0  
Class I  
eDRFSection 0000-0112-6090 R0  
January 2010

*Non-Proprietary Information*

Licensing Topical Report

# **MARATHON-ULTRA CONTROL ROD ASSEMBLY**

*Copyright 2010 GE-Hitachi Nuclear Energy Americas LLC*

## INFORMATION NOTICE

This is a non-proprietary version of the document NEDE-33284P Supplement 1, Revision 0, which has the proprietary information removed. Portions of the document that have been removed are indicated by an open and closed bracket as shown here [[ ]].

## IMPORTANT NOTICE REGARDING THE CONTENTS OF THIS REPORT

### Please Read Carefully

The information contained in this document is furnished **for the purpose of obtaining NRC approval for the use of the Marathon-Ultra control rod in Boiling Water Reactors**. The only undertakings of GE-Hitachi Nuclear Energy (GEH) with respect to information in this document are contained in contracts between GEH and any participating utilities, and nothing contained in this document shall be construed as changing those contracts. The use of this information by anyone other than that for which it is intended is not authorized; and with respect to **any unauthorized use**, GEH makes no representation or warranty, and assumes no liability as to the completeness, accuracy, or usefulness of the information contained in this document.

Copyright 2010, GE-Hitachi Nuclear Energy Americas LLC, All Rights Reserved

## Table Of Contents

|   |      |
|---|------|
| Acronyms And Abbreviations .....                                      | ix   |
| Executive Summary .....   | x    |
| 1. INTRODUCTION AND BACKGROUND.....                                   | 1-1  |
| 2. DESIGN CHANGE DESCRIPTION .....                                    | 2-1  |
| 2.1 Hafnium Application .....   | 2-1  |
| 2.2 Capsule Geometry .....  | 2-1  |
| 3. SYSTEM DESIGN .....  | 3-1  |
| 3.1 Analysis Method.....  | 3-1  |
| 3.1.1 Combined Loading .....  | 3-1  |
| 3.1.2 Unirradiated Versus Irradiated Material Properties .....        | 3-1  |
| 3.2 Material Property Limits .....                                    | 3-2  |
| 3.2.1 Stress Criteria .....   | 3-2  |
| 3.2.2 Welded Connections.....   | 3-2  |
| 3.3 SCRAM .....   | 3-2  |
| 3.4 Seismic and fuel channel bow induced bending.....                 | 3-3  |
| 3.4.1 Wing Outer Edge Bending .....                                   | 3-3  |
| 3.4.2 Absorber Tube to Tie Rod Weld .....                             | 3-3  |
| 3.4.3 Absorber Tube Lateral Load.....                                 | 3-4  |
| 3.4.4 Marathon-5S / Marathon-Ultra Seismic Scram Tests .....          | 3-4  |
| 3.5 Stuck Rod Compression .....                                       | 3-5  |
| 3.6 Absorber Burn-Up Related Loads .....                              | 3-5  |
| 3.6.1 Irradiated Boron Carbide Swelling Design Basis.....             | 3-6  |
| 3.6.2 Clearance Between Capsule and Absorber Tube .....               | 3-6  |
| 3.6.3 Thermal Analysis and Helium Release Fraction .....              | 3-7  |
| 3.6.4 Absorber Tube Pressurization Capability.....                    | 3-8  |
| 3.6.5 Hafnium Application .....                                       | 3-11 |
| 3.6.6 Irradiation Assisted Stress Corrosion Cracking Resistance ..... | 3-13 |
| 3.7 Handling Loads.....   | 3-13 |
| 3.8 Load Combinations and Fatigue.....                                | 3-13 |
| 4. NUCLEAR EVALUATIONS.....   | 4-1  |
| 4.1 Design criteria.....  | 4-1  |
| 4.2 Methodology.....  | 4-1  |
| 4.3 Control Rod Nuclear Lifetime .....                                | 4-2  |
| 4.4 Initial Control Rod Worth.....                                    | 4-3  |
| 4.5 Heat Generation Rates .....                                       | 4-3  |

NEDO-33284 Supplement 1 Revision 0  
Non-Proprietary Information

|   |      |
|---|------|
| 4.6 Control Rod Mechanical Lifetime .....                             | 4-3  |
| 5. OPERATIONAL EVALUATIONS .....                                      | 5-1  |
| 5.1 Dimensional Compatibility .....                                   | 5-1  |
| 5.2 Scram Times .....   | 5-1  |
| 5.3 ‘No Settle’ Characteristics .....                                 | 5-1  |
| 5.4 Drop Speeds .....   | 5-2  |
| 5.5 Fuel Cell Thermal Hydraulics .....                                | 5-2  |
| 6. LICENSING CRITERIA .....   | 6-1  |
| 6.1 Stress, Strain, and Fatigue .....                                 | 6-1  |
| 6.1.1 Criteria .....  | 6-1  |
| 6.1.2 Conformance .....   | 6-1  |
| 6.2 Control Rod Insertion .....                                       | 6-1  |
| 6.2.1 Criteria .....  | 6-1  |
| 6.2.2 Conformance .....   | 6-1  |
| 6.3 Control Rod Material .....  | 6-2  |
| 6.3.1 Criteria .....  | 6-2  |
| 6.3.2 Conformance .....   | 6-2  |
| 6.4 Reactivity .....  | 6-2  |
| 6.4.1 Criteria .....  | 6-2  |
| 6.4.2 Conformance .....   | 6-2  |
| 6.5 Surveillance .....  | 6-3  |
| 6.5.1 Criteria .....  | 6-3  |
| 6.5.2 Conformance .....   | 6-3  |
| 7. EFFECT ON STANDARD PLANT TECHNICAL SPECIFICATIONS .....            | 7-1  |
| 8. PLANT OPERATIONAL CHANGES .....                                    | 8-1  |
| 9. EFFECTS ON SAFETY ANALYSES AND DESIGN BASIS ANALYSIS MODELS ..     | 9-1  |
| 9.1 Anticipated Operational Occurrences and Other Malfunctions .....  | 9-1  |
| 9.2 Accidents .....   | 9-1  |
| 9.3 Special Events .....  | 9-2  |
| 9.4 Fission Product Barrier Design Basis Limits .....                 | 9-2  |
| 9.5 Safety and Design Basis Analysis Models .....                     | 9-2  |
| 10. ABSORBER LOADING OPTIONS .....                                    | 10-1 |
| 11. ABWR AND ESBWR DESIGNS .....                                      | 11-1 |
| 12. SUMMARY AND CONCLUSIONS .....                                     | 12-1 |
| 13. REFERENCES .....  | 13-1 |
| APPENDIX A – FAILED BUFFER SCRAM STRESS EVALUATION .....              | A-1  |
| A-1 Socket Minimum Cross-Sectional Area (Figure 3-1) .....            | A-1  |
| A-2 Velocity Limiter Transition Socket to Fin Weld (Figure 3-1) ..... | A-1  |

NEDO-33284 Supplement 1 Revision 0  
Non-Proprietary Information

|  |     |
|--|-----|
| A-3 Velocity Limiter Fin Minimum Cross-Sectional Area (Figure 3-1) ..... | A-1 |
| A-4 Velocity Limiter to Absorber Section Weld (Figure 3-2) .....         | A-1 |
| A-5 Absorber Section (Figure 3-2).....                                   | A-2 |
| A-6 Absorber Section to Handle Weld (Figure 3-2) .....                   | A-2 |
| A-7 Handle Minimum Cross-Sectional Area (Figure 3-2).....                | A-2 |

**List of Tables**

Table 2-1 Comparison of Typical Parameters of Marathon-5S and Marathon-Ultra CRBs

Table 3-1 Marathon-Ultra Material Properties

Table 3-2 Design Allowable Stresses for Primary Loads

Table 3-3 Weld Quality Factors

Table 3-4 Maximum Control Rod Failed Buffer Dynamic Loads

Table 3-5 D Lattice BWR/2-4 Failed Buffer Scram Stresses

Table 3-6 C Lattice BWR/4-5 Failed Buffer Scram Stresses

Table 3-7 S Lattice BWR/6 Failed Buffer Scram Stresses

Table 3-8 Outer Edge Bending Strain due to Seismic and Channel Bow Bending, Internal Absorber Tube Pressure and Failed Buffer Scram

Table 3-9 Absorber Tube to Tie Rod Weld Stress

Table 3-10 Stuck Rod Compression Buckling – Entire Control Rod (Mode A)

Table 3-11 Stuck Rod Compression Buckling – Control Rod Wing (Mode B)

Table 3-12 Boron Carbide Peak Temperatures

Table 3-13 Handle Lifting Load Stress

Table 3-14 Fatigue Usage due to Failed Buffer Scram

Table 3-15 Fatigue Usage at Absorber Section Outer Edge

Table 3-16 Fatigue Usage at Absorber Tube to Tie Rod Weld

Table 3-17 Hafnium Rod Dimensions

Table 3-18 Irradiated Boron Carbide Capsule Swelling Calculation

Table 3-19 Absorber Tube Pressurization Results: Minimum Material Condition with OD and ID Surface Defects

Table 3-20 Absorber Tube Pressurization Results: Principle Stress Results at Operating Temperature and Pressure and Maximum Allowable Pressure

Table 3-21 D/S Lattice Burst Pressure Results from FEA and Testing

Table 3-22 D/S Lattice Thermal Analysis Results

Table 3-23 C Lattice Thermal Analysis Results

Table 3-24 Finite Element Analysis Summary

Table 4-1 D Lattice Depletion Calculation Results

Table 4-2 C Lattice Depletion Calculation Results

Table 4-3 S Lattice Depletion Calculation Results

NEDO-33284 Supplement 1 Revision 0  
Non-Proprietary Information

Table 4-4 Marathon-Ultra Control Rod Nuclear and Mechanical Depletion Limits

Table 4-5 Heat Generation Rates

Table 4-6 Initial Reactivity Worth, D Lattice (BWR/2-4) Original Equipment and Marathon-Ultra CRBs

Table 4-7 Initial Reactivity Worth, C Lattice (BWR/4,5) Original Equipment and Marathon-Ultra CRBs

Table 4-8 Initial Reactivity Worth, S Lattice (BWR/6) Original Equipment and Marathon-Ultra CRBs

Table 4-9 D Lattice Mechanical Lifetime Calculation

Table 4-10 C Lattice Mechanical Lifetime Calculation

Table 4-11 S Lattice Mechanical Lifetime Calculation

Table 4-12 Boron Carbide Ring Radii in MCNP Model

Table 4-13 D Lattice Original Equipment and Marathon-Ultra Dimensions

Table 4-14 C Lattice Original Equipment and Marathon-Ultra Dimensions

Table 4-15 S Lattice Original Equipment and Marathon-Ultra Dimensions

Table 6-1 Marathon-5S / Marathon-Ultra Nuclear Lifetime Comparison

Table A-1 Socket Axial Stress Calculations

Table A-2 Transition Socket to Fin Weld Stress Calculations

Table A-3 Minimum Fin Area Stress Calculations

Table A-4 Velocity Limiter to Absorber Section Weld Geometry

Table A-5 Velocity Limiter to Absorber Section Weld Stress Calculations

Table A-6 Absorber Section Geometry Calculation

Table A-7 Absorber Section Stress Calculation

Table A-8 Absorber Section to Handle Weld Area Calculation

Table A-9 Absorber Section to Handle Weld Stress Calculations

Table A-10 Handle Scram Stress Calculations

### List of Figures

- Figure 2-1. Marathon-Ultra CRB Absorber Tube Geometry
- Figure 2-2. Marathon-Ultra Absorber Wing Weld Locations
- Figure 2-3. BWR/2-4 D Lattice Marathon-Ultra Control Rod
- Figure 2-4. BWR/4,5 C Lattice Marathon-Ultra Control Rod
- Figure 2-5. BWR/6 S Lattice Marathon-Ultra Control Rod
- Figure 3-1. Velocity Limiter Welds and Cross-Sections Analyzed
- Figure 3-2. Control Rod Assembly Welds and Cross-Sections Analyzed
- Figure 3-3. Absorber Tube to Tie Rod Finite Element Model
- Figure 3-4. Lateral Load Finite Element Model
- Figure 3-5. Lateral Load Finite Element Results (C Lattice)
- Figure 3-6. Control Rod Buckling Modes
- Figure 3-7. Absorber Tube Pressurization Finite Element Model
- Figure 3-8. Absorber Tube and Capsule Thermal Finite Element Model
- Figure 3-9. Handle Lifting Loads Finite Element Model
- Figure 3-10. D/S Lattice Thermal Analysis Results
- Figure 3-11. C Lattice Thermal Analysis Results
- Figure 3-12. Stress Intensity Distribution for Multiple Tube Pressurization Finite Element Model, All Tubes Pressurized
- Figure 3-13. Absorber Tube Burst Pressure Test Specimen – After Test
- Figure 3-14. Absorber Tube Burst Pressure Test Specimen Rupture
- Figure 3-15. Irradiated Boron Carbide Diametral Swelling Data
- Figure 3-16. Irradiated Hafnium Diameter Data
- Figure 4-1. D Lattice Fuel Bundle Rod Position and Enrichment
- Figure 4-2. C Lattice Fuel Bundle Rod Position and Enrichment
- Figure 4-3. S Lattice Fuel Bundle Rod Position and Enrichment
- Figure 4-4. D Lattice Control Rod Cold Worth Reduction with Average Depletion
- Figure 4-5. C Lattice Control Rod Cold Worth Reduction with Average Depletion
- Figure 4-6. S Lattice Control Rod Cold Worth Reduction with Average Depletion
- Figure 4-7. BWR/2-6 Original Equipment

## ACRONYMS AND ABBREVIATIONS

| <b>Acronym /<br/>Abbreviation</b> | <b>Description</b>                             |
|-----------------------------------|--|
| AOO                               | Anticipated operational occurrence             |
| ASME                              | American Society of Mechanical Engineers       |
| ATWS                              | Anticipated Transient Without Scram            |
| CFR                               | Code of Federal Regulations                    |
| CRB                               | Control rod blade                              |
| CRD                               | Control rod drive                              |
| CRDA                              | Control Rod Drop Accident                      |
| ECCS                              | Emergency core cooling system(s)               |
| ECP                               | Engineering Computer Code                      |
| ESF                               | Engineered Safety Feature                      |
| FHA                               | Fuel Handling Accident                         |
| GEH                               | General Electric Hitachi Nuclear Energy        |
| GNF                               | Global Nuclear Fuels                           |
| IASCC                             | Irradiation Assisted Stress Corrosion Cracking |
| LOCA                              | Loss of Coolant Accident                       |
| LTR                               | Licensing topical report                       |
| MCPR                              | Minimum Critical Power Ratio                   |
| MSLBA                             | Main Steamline Break Accident                  |
| NRC                               | U.S. Nuclear Regulatory Commission             |
| OBE                               | Operating Basis Earthquake                     |
| QA                                | Quality assurance                              |
| RAI                               | Request for additional information             |
| SRSS                              | Square root sum of squares                     |
| SSE                               | Safe Shutdown Earthquake                       |
| STS                               | Standard Technical Specifications              |
| TS                                | Technical Specifications                       |

## EXECUTIVE SUMMARY

The GEH Marathon-Ultra control rod is a derivative of the Marathon-5S design approved by Reference 1. The only difference between the Marathon-Ultra and the Marathon-5S design is the absorber section load pattern. Where the Marathon-5S is an all-boron carbide capsule design, the Marathon-Ultra incorporates full-length hafnium rods in outer edge, high depletion tube locations. The geometry and composition of these hafnium rods is identical to those used in the Marathon design, approved in Reference 2. In addition, to maximize the neutron absorber mass, thin-wall capsules are used, with a similar wall thickness to the capsules in the Marathon design (Reference 2).

Like the Marathon-5S capsules, the outer diameter of the Marathon-Ultra capsules is sized [[

]]

A nuclear evaluation of the Marathon-Ultra control rod shows that the initial cold and hot reactivity worths are within  $\pm 5\%$  of the original equipment control rod (“matched worth criteria”). Therefore, the Marathon-Ultra is a direct nuclear replacement for previous control rod designs, and no special nuclear calculation or BWR plant change is required.

The outer structure of the Marathon-Ultra control rod, which is identical to the Marathon-5S control rod, has been evaluated during all normal and upset conditions, and has been found to be mechanically acceptable. The fatigue usage of the control rod has also been found to be well below lifetime limits.

[[

]]

For all cases, the mechanical lifetime exceeds the nuclear lifetime. Therefore, the Marathon-Ultra control rod is nuclear lifetime limited.

The operational performance of the Marathon-Ultra is also evaluated. The scram time, no settle characteristics, and control rod drop speeds are all better than or equal to the original Marathon design. Installation of Marathon-Ultra control rods does not affect any item in the Standard Plant Technical Specifications, and no plant operational change is required. Further, there is no effect on plant safety analyses or on design basis analysis models.

The licensing acceptance criteria applied to the original Marathon and Marathon-5S designs in References 1 and 2 are re-evaluated and are judged to be sufficient and complete. Therefore, the Marathon-Ultra is evaluated against the licensing acceptance criteria in References 1 and 2, and is found to be acceptable. GEH concludes that the new absorber loading of the Marathon-Ultra control rod, combined with the same outer structure as the Marathon-5S control rod approved in Reference 1, is justified for use in Boiling Water Reactors. GEH therefore requests NRC approval for the use of Marathon-Ultra control rods in Boiling Water Reactors.

## 1. INTRODUCTION AND BACKGROUND

GEH currently manufactures Marathon and Marathon-5S Control Rods. The Nuclear Regulatory Commission's (NRC) acceptance of the Marathon-5S Control Rod is documented by a Licensing Topical Report (LTR), Reference 1. The Marathon-5S Control Rod consists of 'simplified' absorber tubes, edge welded together to form the control rod wings, and welded to a full-length tie rod to form the cruciform assembly shape. The absorber tubes are filled with a combination of boron carbide ( $B_4C$ ) capsules, and empty capsules. The previously approved Marathon Control Rod design was approved by the NRC in Reference 2. This control rod consists of 'square' absorber tubes, edge welded together, and welded to individual tie rod segments to form the cruciform assembly shape.

The Marathon-Ultra is a derivative version of the Marathon-5S control rod in that it uses an identical outer structure. The only differences for the Marathon-Ultra is the inclusion of full-length hafnium rods in high-depletion absorber tubes, and the use of a thin-wall boron carbide capsule, similar in geometry to the Marathon control rod design.

Potential effects of the proposed change are evaluated to ensure

- (i) the integrity of the reactor coolant pressure boundary;
- (ii) the capability to shut down the reactor and maintain it in a safe shutdown condition; and
- (iii) the capability to prevent or mitigate the consequences of accidents which could result in potential offsite exposures comparable to the applicable guideline exposures set forth in 10 CFR 50.34(a)(1) and 10 CFR 100.11.

The following sections address the potential effect of the proposed changes on fission product barriers (e.g., fuel cladding) and other involved structures, systems and components, safety functions, design basis events, special events and Standard Technical Specifications (STS) to ensure continued compliance with design and regulatory acceptance criteria.

GEH requests NRC approval for the use of Marathon-Ultra control rods in Boiling Water Reactors.

## 2. DESIGN CHANGE DESCRIPTION

The only difference between the Marathon-Ultra and the Marathon-5S approved by Reference 1, is the absorber section neutron absorber components. The outer structure of the control rod, consisting of the handle, absorber tubes, tie rod, and velocity limiter are identical (Figures 2-3 through 2-5). The component materials and manufacturing processes, including welding, are exactly the same. The simplified absorber tube and capsule configuration is shown in Figure 2-1. The absorber section shell structure is shown in Figure 2-2.

### 2.1 HAFNIUM APPLICATION

Like the Marathon control rod (Reference 2), the Marathon-Ultra control rod employs hafnium rods as a neutron absorber in high duty tube locations. The geometry of the hafnium rods, including diameter, is identical to those used in the Marathon design. As in tubes containing boron carbide capsules, a diametral gap is provided between the hafnium rods and the outer absorber tube to accommodate any possible expansion of the hafnium rod.

Section 3.6.5 provides further evaluation of hafnium for the Marathon-Ultra assembly. This includes a discussion of in-reactor tests that have shown insignificant hydriding of hafnium under BWR conditions, and an expansion calculation demonstrating clearance between the hafnium rod and the outer absorber tube at end of life. Further, the successful application of hafnium in the original Marathon design (Reference 2) is discussed.

### 2.2 CAPSULE GEOMETRY

The Marathon-Ultra control rod uses a thin-wall capsule, similar to the Marathon design approved in Reference 2. As shown in Table 2-1, the Marathon-Ultra uses a [[ ]] nominal wall-thickness capsule. This is comparable to the [[ ]] nominal wall-thickness capsules used in the original Marathon design (Reference 2).

The Marathon-Ultra capsules use the same crimped end cap connection as the Marathon and Marathon-5S designs. The capsule body tube and end cap materials are the same, as is the compacted boron carbide density.

Like the Marathon-5S design, the capsule of the Marathon-Ultra design is sized [[

Section 3.6.2 for a more detailed analysis.

]] See

**Table 2-1**  
**Comparison of Typical Parameters of Marathon-5S and Marathon-Ultra CRBs**

| Parameter                                   | BWR/2-4<br>D Lattice     |                | BWR/4-5<br>C Lattice     |                | BWR/6<br>S Lattice       |                |
|---|--------------------------|----------------|--------------------------|----------------|--------------------------|----------------|
|   | M-5S<br>CRB <sup>1</sup> | M-Ultra<br>CRB | M-5S<br>CRB <sup>1</sup> | M-Ultra<br>CRB | M-5S<br>CRB <sup>1</sup> | M-Ultra<br>CRB |
| Control Rod Weight (lb) <sup>2</sup>        | [[                       |                |                          |                |                          |                |
| Absorber Tubes per Wing                     |                          |                |                          |                |                          |                |
| Nominal Wing Thickness (in)                 |                          |                |                          |                |                          | ]]             |
| <b>Absorber Tube</b>                        |                          |                |                          |                |                          |                |
| Length (in)                                 | [[                       |                |                          |                |                          |                |
| Inside Diameter (in)                        |                          |                |                          |                |                          |                |
| Nominal Thin Section<br>Wall Thickness (in) |                          |                |                          |                |                          | ]]             |
| Material                                    | 304S                     | 304S           | 304S                     | 304S           | 304S                     | 304S           |
| Cross-sectional area (in <sup>2</sup> )     | [[                       |                |                          |                |                          | ]]             |
| <b>B<sub>4</sub>C Absorber Capsule</b>      |                          |                |                          |                |                          |                |
| Length (in)                                 | [[                       |                |                          |                |                          |                |
| Inside Diameter (in)                        |                          |                |                          |                |                          |                |
| Wall Thickness (in)                         |                          |                |                          |                |                          |                |
| Material                                    |                          |                |                          |                |                          |                |
| B <sub>4</sub> C Density (g/cc)             |                          |                |                          |                |                          |                |
| B <sub>4</sub> C Density<br>(% theoretical) |                          |                |                          |                |                          | ]]             |
| <b>Hafnium Rods</b>                         |                          |                |                          |                |                          |                |
| Length (in)                                 | [[                       |                |                          |                |                          |                |
| Diameter (in)                               |                          |                |                          |                |                          |                |
| Density (lb/in <sup>3</sup> )               |                          |                |                          |                |                          | ]]             |

1. Values from Table 2-1 of the Marathon-5S LTR (Reference 1).
2. For 'no settle' and scram considerations, the Marathon-Ultra CRB has been designed to have dry and wet weights that are within the range of previously supplied Marathon and Marathon-5S control rod designs.

[[

]]

**Figure 2-1. Marathon-Ultra CRB Absorber Tube Geometry**

[[

]]

**Figure 2-2. Marathon-Ultra Absorber Wing Weld Locations**

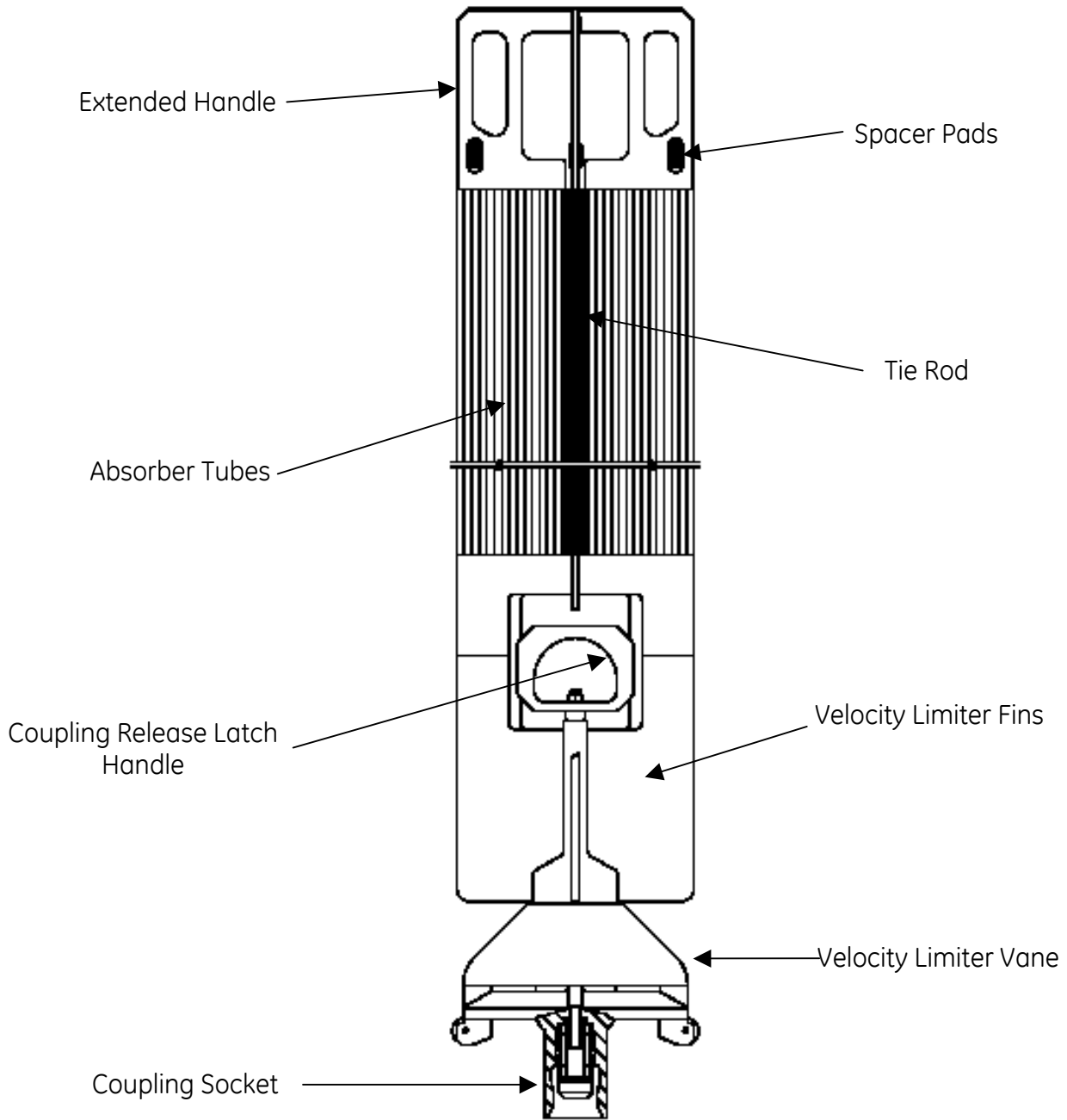


**Figure 2-3. BWR/2-4 D Lattice Marathon-Ultra Control Rod**  
(Extended Handle Shown)

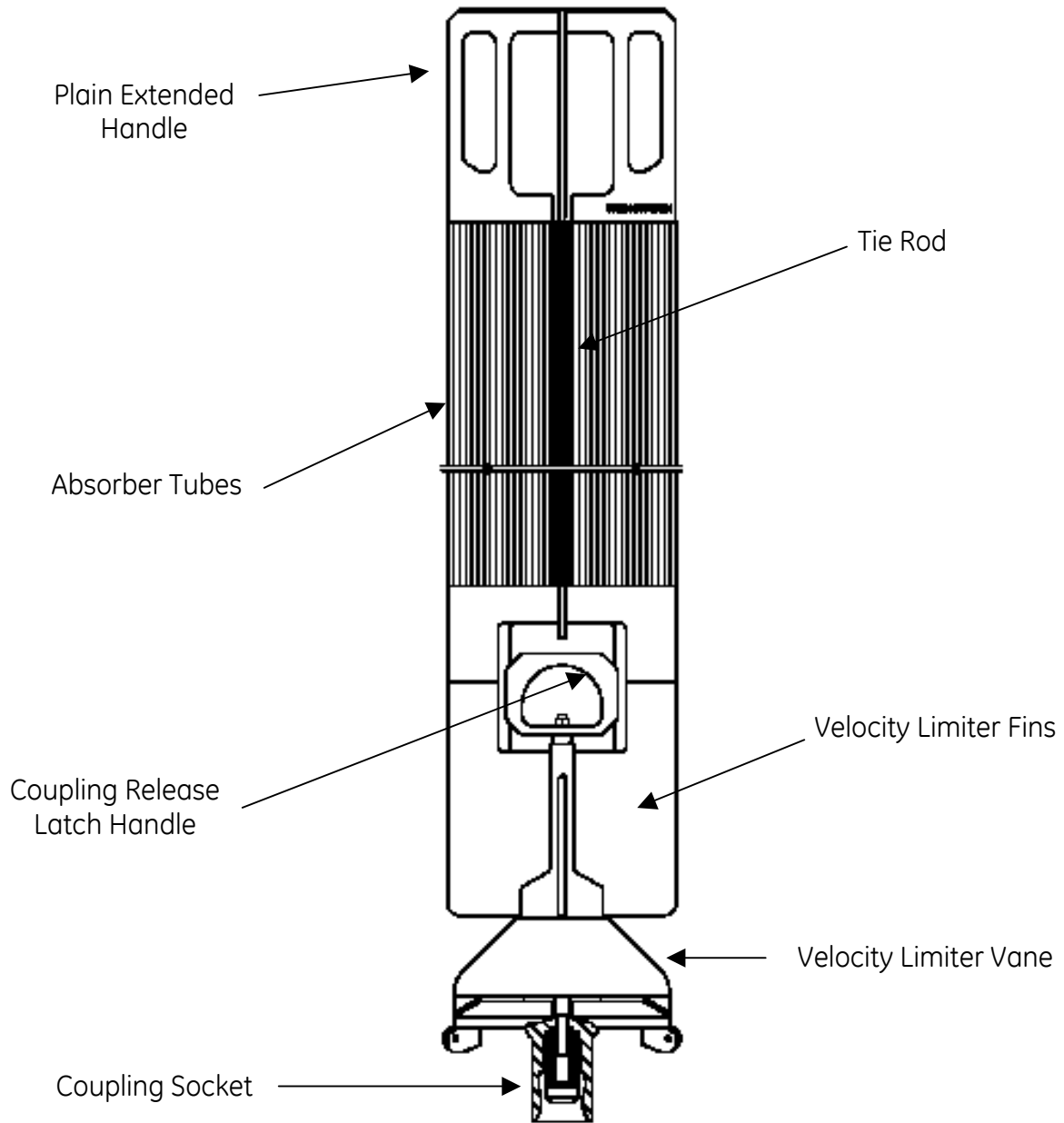


**Figure 2-4. BWR/4,5 C Lattice Marathon-Ultra Control Rod**  
(Extended Handle Shown)

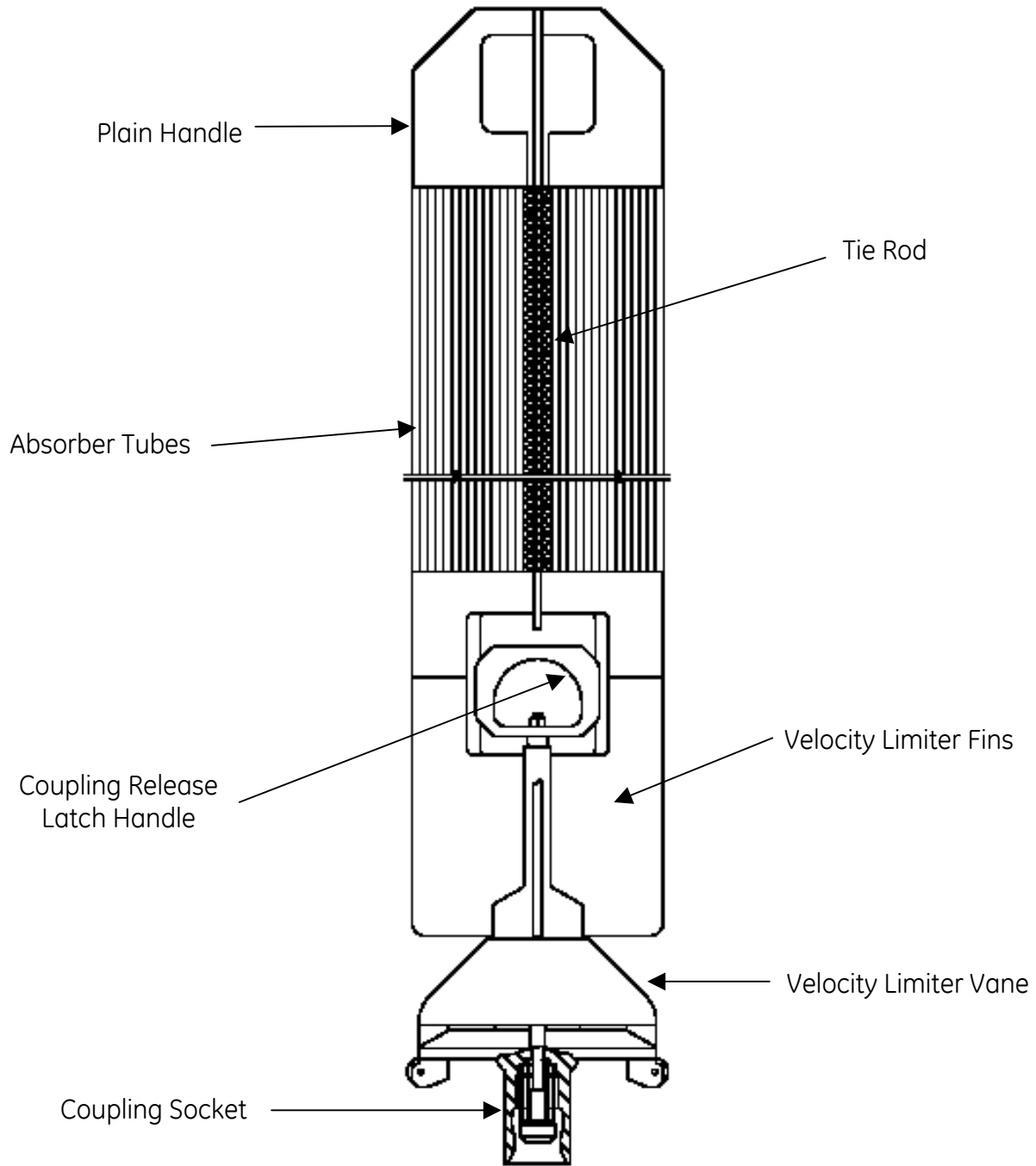


**Figure 2-5. BWR/6 S Lattice Marathon-Ultra Control Rod**

### 3. SYSTEM DESIGN

#### 3.1 ANALYSIS METHOD

For each control rod load application, worst case or bounding loads are identified. Stresses are calculated using worst-case dimensions and limiting material properties. For analyses involving many tolerances, square root sum of squares (SRSS) or statistical tolerancing may be used. Corrosion, wear, and crud deposition are accounted for when appropriate.

It is noted that the analysis methodology for the Marathon-Ultra is identical to the methodology of the Marathon-5S, approved in Reference 1. Furthermore, since the outer structure of the control rods is identical, many of the structural analyses are identical. For example, the material property limits (Section 3.2), seismic and fuel channel bow induced bending (Section 3.4), and stuck rod compression (Section 3.5) analyses are identical to Reference 1. Because of the modified absorber section loading and capsule geometry, the scram loads in Section 3.3, and the absorber burn-up related loads in Section 3.6 are slightly different. However, the analysis methodology and acceptance criteria are identical to that approved in Reference 1.

It is also noted that, since the outer structure of the Marathon-5S and Marathon-Ultra control rods are identical, discussions related to material behavior, metallurgy, manufacturing processes and welding in Reference 1 are equally applicable to the Marathon-Ultra design.

Numerous finite element analyses are used in the design of the Marathon-Ultra control rod, as described in the following sections. Table 3-24 contains a summary of these analyses. As shown in this table, the methodology and finite element model for all of the analyses are identical to those used for the Marathon-5S control rod and approved in Reference 1. Two of the six analyses use slightly different geometry or load inputs applicable to the Marathon-Ultra control rod. The remaining four analyses pertain to the outer structure of the Marathon-Ultra / Marathon-5S control rod, and are completely unchanged.

##### 3.1.1 Combined Loading

As in Reference 1, effective stresses and strains are determined using the distortion energy theory (Von Mises), and compared to allowable limits. Using the principal stresses:  $\sigma_1$ ,  $\sigma_2$ , and  $\sigma_3$ , the equivalent Von Mises stress is calculated as:

$$\sigma_{VM} = \sqrt{1/2[(\sigma_1 - \sigma_2)^2 + (\sigma_2 - \sigma_3)^2 + (\sigma_3 - \sigma_1)^2]}$$

##### 3.1.2 Unirradiated Versus Irradiated Material Properties

Each structural analysis is first evaluated to determine whether unirradiated or irradiated material properties are appropriate. In general, as stainless steel is irradiated, the yield and ultimate tensile strengths increase, while the ductility, or allowable strain decreases. In order to determine the correct technique, the analyses are broken into two categories:

1. Analyses with an applied load (i.e., scram). For these analyses, a maximum stress is calculated, and compared to the limiting unirradiated stress limit.
2. Analyses with an applied displacement (i.e., seismic bending). For these analyses, a maximum strain is calculated, and compared to the limiting irradiated strain limit.

### **3.2 MATERIAL PROPERTY LIMITS**

The limiting unirradiated material strengths are first identified for the control rod structural materials, and shown in Table 3-1. For most materials, limiting values from the ASME Boiler and Pressure Vessel Code are used. In other cases, minimum material strengths are specified in GEH material specifications.

#### **3.2.1 Stress Criteria**

The licensing acceptance criteria of References 1 and 2 are used, in which the control rod stresses and strains and cumulative fatigue shall be evaluated to not exceed the ultimate stress or strain of the material.

The figure of merit employed for the stress-strain limit is the design ratio, where:

$$\text{Design ratio} = \text{effective stress/stress limit, or, effective strain/strain limit.}$$

The design ratio must be less than or equal to 1.0. Conservatism is included in the evaluation by limiting stresses for all primary loads to one-half of the ultimate tensile value.

Resulting allowable stresses for primary loads are shown in Table 3-2.

#### **3.2.2 Welded Connections**

For welded connections, a weld quality factor “q” is used to further reduce the allowable stress. Therefore, the allowable stress for a welded connection,  $S_m'$  is:

$$S_m' = (q) S_m$$

Weld quality factors are determined based on the inspection type and frequency of the weld. Weld quality factors are shown in Table 3-3.

### **3.3 SCRAM**

The methodology for determining maximum control rod loads during a scram event for the Marathon-Ultra control rod is identical to the Marathon-5S methodology approved in Reference 1.

The largest axial structural loads on a control rod blade are experienced during a control rod scram, due to the high terminal velocity. To be conservative, structural analyses of the control rod are performed assuming a 100% failed control rod drive buffer. A dynamic model of mass, spring and gap elements is used to simulate a detailed representation of the load bearing components of the assembly during a scram event. Simulations are run at atmospheric

temperatures, pressures, speeds, and properties as well at operating temperatures, pressures, speeds, and properties. The resulting loads are shown in Table 3-4.

Structural stresses are determined from the scram loads shown in Table 3-4 using the limiting material properties, weld quality factors, and worst-case geometry for the area subject to the load. Figures 3-1 and 3-2 show the welds and cross-sections analyzed.

Resulting maximum stresses during a failed buffer scram are shown in Tables 3-5, 3-6 and 3-7 for D lattice BWR/2-4, C lattice BWR/4-5, and S lattice BWR/6 applications. These stresses are evaluated against the stress limits shown in Table 3-2. Specific details for each calculation are shown in Appendix A. As shown by the design ratios in Tables 3-5 through 3-7, sufficient margin exists against failure for all cross-sections and welds.

### **3.4 SEISMIC AND FUEL CHANNEL BOW INDUCED BENDING**

Fuel channel deflections, which result from seismic events, impose lateral loads on the control rods. The Marathon-Ultra control rod is analyzed for Operating Basis Earthquake (OBE) events and Safe Shutdown Earthquake (SSE) events. It is noted that the contents of this section are the same as that approved for the Marathon-5S in Reference 1, as the outer structure of the control rods is identical.

#### **3.4.1 Wing Outer Edge Bending**

The OBE analysis is performed by evaluating the strain in the Marathon-5S absorber section with maximum OBE deflection. In addition, maximum control rod deflections due to fuel channel bulge and bow are conservatively added to the calculated seismic bending deflections.

[[  
]]

The limiting location for strain due to bending of the control rod cross-section occurs at the outer edge of the control rod wing. At this location, a combined strain due to simultaneous application of the following loads is calculated: (1) control rod bending due to an OBE seismic event, (2) control rod bending due to worst case channel bulge and bow, (3) axial absorber tube stress due to maximum internal pressure, and (4) a failed buffer scram. The results of these strain calculations are shown in Table 3-8. As shown, even under these combined worst-case conditions, the maximum strain is well below the limiting maximum allowable strain at irradiated conditions.

#### **3.4.2 Absorber Tube to Tie Rod Weld**

The combined effect of control rod bending due to OBE and channel bulge and bow deflection combined with maximum absorber tube internal pressure is also evaluated at the full-length tie rod to absorber tube weld. A finite element model is used, as shown in Figure 3-3. Resulting worst-case stresses are shown in Table 3-9. As shown, the resulting stresses are acceptable against the design criteria.

### 3.4.3 Absorber Tube Lateral Load

Finally, the lateral load imposed on the control rod absorber tube due to an excessively bowed channel is evaluated. The finite element model is shown in Figure 3-4. As shown, the entire lateral load is applied to a single square absorber tube, along with reactor internal pressure. For conservatism, no internal pressure is applied to the tube, which would offset the external pressure and reduce the stresses in the tube.

The resulting stress intensity plot is shown in Figure 3-5. The maximum stress intensity is calculated as  $[[ \quad ]]$ , which is less than the absorber tube allowable load of  $[[ \quad ]]$  from Table 3-2.

### 3.4.4 Marathon-5S / Marathon-Ultra Seismic Scram Tests

For the SSE analysis, the control rod must be capable of full insertion during fuel channel deflections. Like the Marathon-5S (Reference 1), because the Marathon-Ultra control rod has a stiffness less than or equal to the Marathon assembly, and because the weight of the Marathon-Ultra control rod is less than previous designs, the Marathon-Ultra has seismic scram capability equal to or better than the Marathon control rod (See Section 5.2).

Seismic scram tests of the Marathon-5S control rod are discussed in Sections 3.4.4 and 5.2 of Reference 1. The parameters affecting seismic scram performance are the bending stiffness of the assembly, and the overall weight of the assembly. In general, a more stiff assembly, and a heavier assembly will have slower seismic scram times. The test specimens used for the Marathon-5S seismic scram tests were purposefully made heavier than production Marathon-5S assemblies as a test conservatism. The weight of production Marathon-Ultra control rod assemblies is also conservatively bound by the weight of the test assemblies. Because the outer structure of the Marathon-Ultra is identical to the Marathon-5S, the lateral bending stiffness will also be identical. Therefore, the Marathon-5S seismic scram tests apply equally to the Marathon-Ultra assemblies.

The test facility used consists of a simulated pressure vessel and reactor internals, and a control rod drive. Prototype control rods were installed, and the control rod drive was set to simulate D, C, and S lattice operation.

The prototypes used for the test incorporated plain, roller-less handles, as described in Appendix A of Reference 1. The acceptance criterion for the test was that scram time requirements were to be met up to fuel bundle oscillation consistent with an OBE (Operational Basis Earthquake) event, and that the control rods would successfully insert under an SSE (Safe Shutdown Earthquake) event. The results of the tests were very successful, in that scram time requirements were met through the much more severe SSE event for both the C lattice and S lattice applications. The D lattice application met scram time requirements with OBE fuel channel deflections, and successfully inserted under SSE conditions. Therefore, the acceptance criteria for the test were met. During the tests, the control rods received very little wear.

### 3.5 STUCK ROD COMPRESSION

Maximum compression loads from the control rod drive (CRD) are evaluated for a stuck control rod. Both buckling, and compressive yield are analyzed for the entire control rod cross-section (buckling mode A), and conservatively assuming that the entire compression load is applied to a single control rod wing (buckling mode B). Figure 3-6 shows the buckling modes. An additional axial load of 600 lb due to channel bulge and bow is also added to the compression load.

Results of the stuck rod compression loads are contained in Table 3-10 for the entire control rod cross-section (mode A), and in Table 3-11 for the single wing (mode B). As can be seen, neither compressive yielding nor buckling will occur for either buckling mode. Additionally, for both buckling modes, the compressive yield load is reached prior to the critical buckling load. This analysis for the Marathon-Ultra control rod is identical to that for the Marathon-5S control rod, approved in Reference 1.

### 3.6 ABSORBER BURN-UP RELATED LOADS

The methodology for evaluating absorber burn-up related loads for the Marathon-Ultra control rod is identical to the Marathon-5S methodology approved in Reference 1. This includes the use of the same irradiated boron carbide swelling design basis, clearance evaluation methodology, thermal analysis methodology, and absorber tube pressurization methodology. There are small differences in the results of the analyses, as a result of the use of the thin-wall capsule body tube. However, the conservative criteria [[  
]]

The structure of a control rod must provide for positioning and containment of the neutron absorber material (boron carbide powder, hafnium, etc) throughout its nuclear and mechanical life and prohibit migration of the absorber out of its containment during normal, abnormal, emergency and faulted conditions. The Marathon-Ultra control rod, like the Marathon and Marathon-5S control rods, contains boron carbide ( $B_4C$ ) powder within capsules contained within absorber tubes (capsule within a tube design).

The boron neutron absorption reaction releases helium atoms. Some of this helium gas is retained within the compacted boron carbide powder matrix, causing the powder column to swell. This swelling causes the  $B_4C$  capsule to expand. The remainder of the helium is released as a gas. Like previous Marathon designs, the capsule end caps for the Marathon-Ultra design are crimped to the capsule body tubes. This allows the helium gas to escape from the capsule and fill the absorber tube gap and any empty capsule plenum volume provided.

For the original Marathon capsule design, [[

]]

Like the Marathon-5S design, the Marathon-Ultra capsule tube dimensions are sized [[

]]

Using the pressurization capability of the absorber tube, limits are determined for each absorber tube configuration, in terms of B<sub>4</sub>C column depletion.

These individual absorber tube depletion limits are then combined with radial depletion profiles and axial depletion profiles to determine the mechanical depletion limit for the control rod assembly (Section 4.6).

### 3.6.1 Irradiated Boron Carbide Swelling Design Basis

Mechanical test data of the irradiated behavior of boron carbide was obtained by irradiating test capsules as described in Reference 1.

As discussed in Reference 11, GEH completed a post-irradiation examination of a Marathon control rod in April 2009. Part of this examination was dimensional measurements related to boron carbide swelling rates. As discussed in Section 6 of Reference 11, these dimensional measurements strongly support the design basis boron carbide swelling rates used in Reference 1 for the Marathon-5S, as the new data very closely matches the existing data. Both sets of data are shown graphically in Figure 3-15. As shown, +3σ upper limit used for the Marathon-5S bounds both sets of data. Therefore, this same conservative design basis swelling used for the Marathon-Ultra control rod design.

### 3.6.2 Clearance Between Capsule and Absorber Tube

As a result of the welding process forming the control rod wings, the inside diameter of the absorber tubes shrink. Therefore, a minimum inside diameter is established, and is 100% inspected following the welding, before the absorber section is loaded with capsules.

The worst-case capsule dimensions are used, which result in the maximum outside diameter at 100% local depletion. These consist of the original maximum outside diameter, and minimum wall thickness, resulting in the maximum beginning boron carbide diameter.

The strain at the ID of the capsule is equal to the diametral strain of the boron carbide powder. The +3σ upper limit of boron carbide swelling data is used. Then, assuming constant volume deformation of the capsule, the strain on the outside diameter of the capsule is:

[[ ]]

Then, the capsule outside diameter at 100% local depletion is:

$$OD_{100\%} = OD_0(1 + \epsilon_{OD}).$$

A summary of this calculation is shown in Table 3-18 for both the D/S lattice and C lattice absorber tube and capsule combinations. [[

]]

### 3.6.3 Thermal Analysis and Helium Release Fraction

The following methodology is identical to that approved for the Marathon-5S in Reference 1. The only difference is that the Marathon-Ultra capsule geometry and heat generation rates are incorporated.

Pressure in the absorber tube due to helium release is calculated accounting for worst-case capsule and absorber tube dimensions and B<sub>4</sub>C helium release fraction. Because the amount of helium released from the B<sub>4</sub>C powder increases with temperature, a finite element thermal analysis is performed to determine the peak B<sub>4</sub>C temperature (see Figure 3-8). This thermal analysis is performed using worst-case dimensions, maximum end-of-life crud buildup, combined with maximum beginning-of-life heat generation.

For the thermal model, corrosion is modeled as the build-up of an insulating layer of crud. This crud may be corrosion products from the control rod absorber tube, or deposited from other reactor internals. For all thermal analyses, a crud layer corresponding to a 32-year residence time is used ([[ ]])

A temperature distribution is shown in Figure 3-8 for the D/S lattice case. The model used assumes that the tube is interior to the wing, in that there is another absorber tube to the left and right. The boundary on the left and right is conservatively assumed to be perfectly insulated (zero heat flux).

Results for both D/S lattice and C lattice are shown in Tables 3-22 and 3-23, and in Figures 3-10 and 3-11. The following conservatisms are applied to the thermal model:

- Peak beginning-of-life heat generation rates are used, these are combined with:
- End-of-life combined corrosion and crud build-up of [[ ]], twice that used in previous analyses.
- Peak heat generation rates are used from the highest heat generation tube, which is actually the outermost edge tube. In reality, this tube will have coolant on one side, rather than be insulated. Further, some heat transfer will occur from the peak heat generation tube to the adjacent tube, rather than be perfectly insulated.
- Maximum wall thickness dimensions are used.

Peak B<sub>4</sub>C temperatures are shown in Table 3-12. The temperatures shown in this table are based on peak beginning-of-life boron carbide heat generation rates (see Section 4.5), and are from the peak heat generation absorber tube at the peak axial location. They are radially averaged only across the cross-section of an individual boron carbide capsule.

Helium release fractions are based on models developed using data from multiple sources. The data shows a significant dependence of helium release fraction on the irradiation temperature. The helium release fractions used for each lattice type are shown in Table 3-12. The helium release model is based on data from 500 °F to 1000 °F, which envelops the temperatures shown in Table 3-12.

### 3.6.4 Absorber Tube Pressurization Capability

As discussed in Section 2, the Marathon-Ultra control rod uses the same ‘simplified’ absorber tube as the Marathon-5S control rod. Therefore, the following analysis of the absorber tube pressurization capability is the same as that in Reference 1.

[[

]]

Finite element analyses are performed to determine the pressurization capability of the absorber tube. These analyses incorporate the use of worst-case dimensions, maximum expected wear, and the largest allowable surface defects (see Figure 3-7).

#### Absorber Tube Defects

The limiting case used for establishment of the absorber tube allowable pressure simultaneously combines worst-case absorber tube dimensions (thinnest wall per drawings), surface defects at the center of the flat portion of the tube, on the round portion of the tube, and a crack-like defect on the thinnest portion of the inside diameter of the tube.

The largest sized allowable surface defects are based on the manufacturing capability of the absorber tube. A collaborative effort was undertaken with the supplier of the absorber tubes to determine a maximum surface defect size that would maintain reasonable yield rates, but would not reduce the pressurization capability of the tube below acceptable values. A surface defect depth limit of [[            ]] in depth was determined, applied to the absorber tubing specification, and factored into the pressurization analysis.

At receipt inspection, the acceptance criteria for surface defects are based primarily on the depth of the defect. Additionally, matching sets of visual standards are used by both the supplier and by GEH to identify acceptable and unacceptable surface features.

The finite element analysis shows that smaller diameter defects result in larger stress concentrations around the defect. A survey was performed of surface defects, and the smallest area defect was found to be [[            ]] in diameter. Therefore, a diameter of [[            ]] was used for the finite element model surface defects.

After factoring in maximum allowable surface defects and worst-case (thinnest wall) absorber tube geometry, the finite element analysis is performed. An example stress distribution is shown in Figure 3-7. The surface defect geometry is also shown.

The burst pressure is defined as the internal pressure at which any point in the tube reaches a stress intensity equal to the true ultimate strength of the material. Then, to calculate an allowable pressure, a safety factor of 2.0 is applied to the differential pressure across the absorber tube wall such that:

$$P_{allow} = \frac{(P_{burst} - P_{external})}{2} + P_{external}$$

The calculated burst and allowable pressures are shown in Table 3-19. The results at operating temperature are limiting, and are used as the design basis allowable pressure of the tubes.

#### Absorber Tube Wear and Corrosion

Corrosion and wear are significant to the pressurization capability analysis of the absorber tube. In the pressurization analysis, the peak stress concentrations occur on the 'flat' portion of the tube. Combined corrosion and wear on this surface are modeled as a removal of material.

The analysis shows that combined corrosion and wear, modeled as a removal of material for the pressurization analysis, can exceed [[ ]] without affecting the design basis allowable pressure of the outer absorber tube shown in Table 3-19. For the D/S lattice absorber tube, the upper limit for combined corrosion and wear that occurs after control rod installation is [[ ]] For the C lattice absorber tube, the upper limit is [[ ]] This amount of wear is considered sufficiently conservative.

#### Maximum Stress Components

Stress components at the point of maximum stress intensity were analyzed for the absorber tube with the maximum allowable internal pressure. The point of maximum stress intensity is found to be on the outer edge of the absorber tube, at the middle of the flat portion. Principle stress components are shown in Table 3-20. All stress values shown in Table 3-20 are within the allowable stress value for 304S tubing of [[ ]] shown in Table 3-2.

#### Effect of the Welded Connection Between Absorber Tubes

The effect of the welded connection between adjacent absorber tubes on the stresses in the tube due to internal pressure was evaluated using a multiple tube finite element model. In this model, three adjacent absorber tubes were pressurized. A stress intensity distribution is shown in Figure 3-12. As shown, the maximum stress is at the flat portion of the tube exposed to the coolant. The effect of the adjacent pressurized tubes is to produce compressive rather than tensile stresses in the flat portions of the tube that are welded together. In this way, the opposing pressures from opposite sides of this welded ligament is actually beneficial in terms of the pressurization capability of the tubes.

A comparison of this multiple tube model to the single tube model showed that the single tube model predicts lower burst pressures. Therefore, the single tube model is used to determine design basis allowable pressures, and there is no degrading effect due to the lack of gaps between the absorber tubes in the Marathon-Ultra design.

The Marathon-5S and Marathon-Ultra Control Rod Blades (CRB) are manufactured using very low heat input laser weld processes. The resulting regions of microstructural change including the associated heat affected zones (HAZ) are very small (see Section 3.2). Based on general understanding, the fine HAZ microstructure will have mechanical properties that are equivalent to, or exceed, those of the wrought base material. Therefore, the HAZ will have mechanical properties that exceed the required minimum properties of the associated wrought material.

Two potential issues arise from welding of the absorber section: (1) sensitization and (2) residual stress. These issues are addressed below:

*Sensitization:* The low heat input laser welding processes have minimal impact on the wrought tube material, in that they typically do not result in sensitized material. To confirm this conclusion, the processes are continually evaluated metallographically to confirm the acceptability of the weld region (i.e., lack of sensitization). [[

]] Note also from Section 3.6.2 that these contact hoop stresses (and associated strains) have been eliminated for the Marathon-Ultra control rod.

*Residual stress:* One major effect of the welding process is that it will introduce tensile residual stresses in the narrow weld/HAZ region. These stresses are not a significant concern for two reasons: (1) The field cracking has not been associated with the weld HAZ and (2) the irradiation experienced by the CRB over the initial time of operation can significantly reduce these stresses by 60% or more through radiation creep processes (Reference 8). At this level of reduced stress, there is little concern for any effect on stress corrosion cracking (SCC) initiation or their applied stresses and strains. In that the major concern are strains from swelling, this level of stress is well below those levels required to even produce yielding (see also Section 3.2).

#### Effect of Irradiated Material

The pressurization finite element model uses unirradiated material properties. To test the assertion that the use of unirradiated properties in the pressurization finite element model is conservative, a test case is performed. The D lattice, 550 °F case is chosen for the test, with worst-case dimensions and maximum allowable surface defects. An internal pressure of [[ ]]

]] is applied, which is the burst pressure found using unirradiated materials, as shown in Table 3-19. At this internal pressure, the maximum stress intensity using irradiated materials is [[ ]], which is less than the true ultimate strength of the irradiated material, [[ ]]. Therefore, since the test case using irradiated material properties does not reach the ultimate strength of the irradiated material, the burst pressure analysis using unirradiated material properties is conservative. Further, the maximum strain intensity in the tube for the irradiated property test is low, at [[ ]].

#### Burst Pressure Tests

As discussed above, the allowable pressure for the absorber tube for the Marathon-Ultra is based on a finite element model incorporating worst-case dimensions, along with maximum specification permitted surface defects and expected wear. The finite element analysis shows that the worst-case burst pressure, on which the allowable pressure of the Marathon-Ultra tube is based, is [[ ]] lower than the burst pressure using nominal dimensions and no surface defects. See Table 3-21.

To confirm the finite element results, burst pressure tests were performed on two test specimens consisting of a short panel of welded absorber tubes, in which all tubes are pressurized, see Figures 3-13 and 3-14. The resulting tested burst pressures are compared to the finite element calculated burst pressures in Table 3-21.

As shown, the test results exceed the nominal predicted burst pressure by approximately [[ ]], and exceed the worst-case burst pressure (worst-case dimensions and surface defects) by a wide margin ([[ ]]). Since the design basis allowable pressure for the absorber tube is based on the worst-case burst pressure combined with a safety factor of 2.0, the design is conservative.

### Conclusions

The analysis is conservative because it considers the combined effects of: (1) worst case tube dimensions (thinnest wall), (2) maximum allowable surface defects, (3) a large amount of combined corrosion and wear, and (4) unirradiated material properties. The true ultimate strength of the material will increase with irradiation. Burst pressure tests further validate the design basis allowable pressures.

### **3.6.5 Hafnium Application**

As discussed in Section 2.1, the Marathon-Ultra incorporates hafnium rods as a neutron absorber in high-duty absorber tube locations. The configuration of the hafnium rods, including hafnium material requirements, diameter and length, are identical to the hafnium rods currently used in the original Marathon design (Reference 2).

GEH has a long, successful history of using hafnium as a neutron absorber in both DuraLife and Marathon control rods (Reference 2). In the Marathon design in particular, the hafnium rods are sealed from reactor coolant within the outer absorber tube. [[

]] The inspection history of the application of hafnium rods to the Marathon design is very good, in that for all inspections of irradiated Marathon control rods contained in Reference 10, no material failures have been observed in any absorber tubes containing hafnium rods.

The diameters of the hafnium rods, the maximum hafnium rod diameter after thermal expansion, and the minimum absorber tube inside diameters are shown in Table 3-17. As shown, there is a large diametral gap between the hafnium and the absorber tube that allows for any expansion of the hafnium rod, ensuring that no strain is placed on the outer absorber tube.

### Hydrogen Hydriding

Issues with the hydriding of hafnium have been observed in PWR applications (Reference 9). Hydriding involves hydrogen from the reactor coolant permeating the outer stainless steel tubing, and reacting with the hafnium to form hafnium hydride. Since hafnium hydride has a higher specific volume than hafnium, the hafnium rod may swell. The effect of the hydriding in PWRs has typically been observed as localized blisters or bulges on the surface of the hafnium rods, which place a strain on the outer cladding of the control assembly.

To investigate the occurrence of the hydriding phenomenon under lower pressure BWR conditions, a test was performed. In this test, two D lattice square absorber tube sections, with 6" long hafnium rods sealed inside, were loaded into a 'dummy' neutron source holder irradiation capsule, and irradiated for two, twelve month cycles in a BWR. The accumulated fast fluence was  $1.6$  to  $2.4 \times 10^{21}$  n/cm<sup>2</sup> (E > 1MeV).

After the test, hydrogen content of the hafnium test specimens was found to be [[  
]] for both specimens. Archive samples of the same material found initial hydrogen content to be [[  
]]. Therefore, [[

]] The conclusions of this test apply equally to the simplified absorber tube, since the geometry of the tube is not expected to have any effect on the ability of the hydrogen to permeate the stainless steel tube and migrate to the hafnium. This is conservative, as the simplified absorber tube has a larger minimum wall thickness than the square tube. Therefore, if anything, the simplified tube should be less permeable to hydrogen transport.

### Irradiated Hafnium Rod Measurements

GEH completed a Post-Irradiation Examination (PIE) of a highly irradiated Marathon control rod in April 2009 (Reference 11). As part of the on-going investigation, hafnium rods from this control rod were examined. [[

]]

Diameter data from the irradiated hafnium is shown in Figure 3-16. By specification, the hafnium rods used in this control rod were to be between [[  
]] in diameter. It is noted that this is larger than the rods currently used for Marathon control rod and for the Marathon-Ultra control rod ([[  
]]). Figure 3-16 plots the diameter measurements versus the distance from the top of the absorber section. Data on the actual initial diameter of the hafnium rods is not available. However, any irradiation-related expansion phenomenon should be apparent by comparing the diameter at the top of the rod to the diameter at the bottom. This is because the top of the hafnium rod receives significantly more irradiation than the bottom of the rod.

As shown in Figure 3-16, [[

]], it may be concluded that there were no absorber burn-up related stresses or strains placed on the outer absorber tubes containing hafnium rods.

### Conclusions

GEH's experience with the application of hafnium to the Marathon design is very good, with no observed material failures for absorber tubes containing hafnium rods. [[

]] Therefore, it may be concluded that no hafnium irradiation related stresses or strains will be placed on the outer absorber tube for the Marathon-Ultra design.

### 3.6.6 Irradiation Assisted Stress Corrosion Cracking Resistance

In order for the stress corrosion cracking mechanism to activate it requires a material that is susceptible, a conducive environment and a sustained tensile stress. If one of these three mechanisms is not present to a sufficient degree, the likelihood of a stress corrosion crack to form is significantly reduced. These three areas are addressed for the Marathon-Ultra design as follows.

*Susceptible Material:* The Marathon absorber tube is made from a GEH proprietary stainless steel, “Rad Resist 304S”, which is optimized to be resistant to Irradiation Assisted Stress Corrosion Cracking (IASCC). The Marathon-Ultra absorber tubes are also fabricated from this material, and thus, are expected to have the same crack resistant properties. The tubes are delivered by the tubing supplier in a fully annealed condition, minimizing residual stress from the drawing process. Finally, the tubes are welded together using a low heat input laser weld process, resulting in low residual plastic strains and a very small heat affected zone (Section 3.6.4).

*Sustained Tensile Stress:* The Marathon-Ultra is designed such that [[ ]] (see Section 3.6.2). This significantly reduces the amount of stress/strain present in the absorber tubes at the end of life, and significantly reduces the likelihood of stress-corrosion cracking.

*Conducive Environment:* Like the Marathon-5S, the Marathon-Ultra is a completely crevice-free design for the absorber section and handle. All absorber tubes are sealed at the top and bottom, and full-length welds joining the tubes ensure that no crevice condition exists between the tubes. The elimination of handle rollers also ensures that the upper handle is crevice-free.

### 3.7 HANDLING LOADS

As for the Marathon-5S control rod (Reference 1), the Marathon-Ultra control rod is designed to accommodate twice the weight of the control rod during handling, to account for dynamic loads. The handle is analyzed using a finite element model, using worst-case geometry (see Figure 3-9). Table 3-13 shows the results of the handle loads analysis.

### 3.8 LOAD COMBINATIONS AND FATIGUE

The Marathon-Ultra control rod is designed to withstand load combinations including anticipated operational occurrences (AOOs) and fatigue loads associated with those combinations. The fatigue analysis is identical to that approved in Reference 1 for the Marathon-5S, and is based on the following assumed lifetime, which is consistent with previous analyses:

- [[ ]] and
- [[ ]]

For scram, each cycle represents a single scram insertion. Scram simulations show that the oscillations in the control rod structure damp out quickly. Further, it is extremely conservative to assume [[ ]] scrams with a 100% inoperative control rod drive buffer, as the loads experienced by the control rod in a normal buffered scram are much less severe.

NEDO-33284 Supplement 1 Revision 0  
Non-Proprietary Information

For the Operational Basis Earthquake (OBE), with a total of [[     ]] seismic events, each event consists of [[     ]] cycles of control rod lateral bending. The assumption of [[     ]] lifetime OBE events is also considered very conservative.

Based on the reactor cycles, the combined loads are then evaluated for the cumulative effect of maximum cyclic loadings. The fatigue usage is evaluated against a limit of 1.0. The maximum cyclic stress is determined using a conservative stress concentration factor of 3.0. Table 3-14 shows the fatigue usage due to control rod SCRAM at three limiting weld locations. In this analysis, it is assumed that each scram occurs with a 100% failed CRD buffer.

Table 3-15 shows the fatigue usage at the control rod outer edge due to bending from OBE seismic events and severe channel bow, control rod scram, and maximum absorber tube internal pressure. As can be seen, the combined fatigue usage is much less than 1.0.

Table 3-16 shows the fatigue usage at the tie rod to first absorber tube weld. The combined loading due to failed buffer scram, maximum absorber tube internal pressure, OBE seismic events and severe channel bow is considered. As shown, the combined fatigue usage is much less than 1.0.

It is well known that the cycles for fatigue initiation are dependent on the stress or strain range. The number of loading cycles that the control rod blade experience are limited to 100 for all of the different designs. The stress amplitudes are all in the elastic range. As shown in Table 3-14 through Table 3-16, based upon the ASME Section III fatigue design curve for un-irradiated austenitic material (Reference 6), the low number of cycles represents only a small amount of cumulative damage, well below the design limit. The  $\frac{1}{2}$  ultimate tensile stress value represents the ASME design limit for  $\sim 30,000$  cycles. It has been established that an increase in the strength level, consistent with the effect of irradiation, would only increase the margin. This is supported by data on high strength materials, which confirm that the endurance limit is close to  $\frac{1}{2}$  ultimate tensile stress (Reference 7).

The last consideration with regard to fatigue is an evaluation of whether there is any flow-induced vibration that could in turn provide the potential for fatigue initiation. An assessment was performed to evaluate the loads induced by transverse loading. The evaluation that treated the control blade as a cantilever beam, found that the loads were very small and would not be sufficient to even close the gap between the blade and the fuel assembly. This load is considered so small as to be negligible, and would not lead to any risk of fatigue.

**Table 3-1  
 Marathon-Ultra Material Properties**

| Material Type        | Control Rod Components                                       | Ultimate Tensile Strength, S <sub>U</sub> (ksi) |        | Yield Strength, S <sub>Y</sub> (ksi) |        | Modulus of Elasticity, E (x 10 <sup>6</sup> psi) |        | Poisson's Ratio, ν |        |
|----------------------|--|---|--------|--------------------------------------|--------|--|--------|--------------------|--------|
|                      |  | 70 °F   | 550 °F | 70 °F                                | 550 °F | 70 °F  | 550 °F | 70 °F              | 550 °F |
| 316 Plate            | Handles and pads; VL fins, VL Hardware                       | [[  |        |                                      |        |  |        |                    |        |
| 316 Bar              | Handle pads; VL hardware                                     |   |        |                                      |        |  |        |                    |        |
| XM-19 Bar            | VL socket  |   |        |                                      |        |  |        |                    |        |
| CF3 Casting          | VL vane casting, latch handle casting                        |   |        |                                      |        |  |        |                    |        |
| ER 308L              | Capsule end caps, absorber tube end plugs, weld filler metal |   |        |                                      |        |  |        |                    |        |
| 304S Bar             | Tie rods   |   |        |                                      |        |  |        |                    |        |
| 304S Tubing          | Absorber Tubes   |   |        |                                      |        |  |        |                    |        |
| Hardened 304L Tubing | Capsule body tubes   |   |        |                                      |        |  |        |                    | ]]     |

NEDO-33284 Supplement 1 Revision 0  
Non-Proprietary Information

**Table 3-2  
Design Allowable Stresses for Primary Loads**

| Material Type           | CR Components   | $\frac{1}{2}$ Ultimate Tensile Stress<br>$S_m$ (ksi) |        |
|-------------------------|---|--|--------|
|                         |   | 70 °F  | 550 °F |
| 316 Plate               | Handles and pads;<br>VL fins, VL<br>Hardware                          | [[   |        |
| 316 Bar                 | Handle pads; VL<br>hardware   |  |        |
| XM-19 Bar               | VL transition<br>socket   |  |        |
| CF3 Casting             | VL vane casting,<br>latch handle<br>casting                           |  |        |
| ER 308L                 | Capsule end caps,<br>absorber tube end<br>plugs, weld filler<br>metal |  |        |
| 304S Bar                | Tie rods  |  |        |
| 304S Tubing             | Absorber Tubes  |  |        |
| Hardened 304L<br>Tubing | Capsule body<br>tubes   |  | ]]     |

**Table 3-3  
 Weld Quality Factors**

| <b>Weld</b>                | <b>Weld Inspection</b> | <b>Weld Quality Factor,<br/>q</b> |
|----------------------------|------------------------|-----------------------------------|
| Transition Socket to Fin   | [[                     |                                   |
| Fin to Absorber Section    |                        |                                   |
| Handle to Absorber Section |                        |                                   |
| End Plug to Absorber Tube  |                        |                                   |
| Vane to Transition Piece   |                        | ]]                                |

**Table 3-4  
 Maximum Control Rod Failed Buffer Dynamic Loads**

| <b>Components</b>                 | <b>Maximum Equivalent Loads in Kips (10<sup>3</sup> lbs)<br/>(Tension Listed as Negative)</b> |               |                  |               |                  |               |
|-----------------------------------|---|---------------|------------------|---------------|------------------|---------------|
|                                   | <b>D Lattice</b>  |               | <b>C Lattice</b> |               | <b>S Lattice</b> |               |
|                                   | <b>70 °F</b>  | <b>550 °F</b> | <b>70 °F</b>     | <b>550 °F</b> | <b>70 °F</b>     | <b>550 °F</b> |
| Coupling                          | [[  |               |                  |               |                  |               |
| Velocity Limiter (VL)             |   |               |                  |               |                  |               |
| VL/Absorber Section Interface     |   |               |                  |               |                  |               |
| Absorber Section                  |   |               |                  |               |                  |               |
| Handle/Absorber Section Interface |   |               |                  |               |                  |               |
| Handle                            |   |               |                  |               |                  | ]]            |

**Table 3-5**  
**D Lattice BWR/2-4 Failed Buffer Scram Stresses**

| Location                                  | Room Temperature (70 °F) |                 |              | Operating Temperature (550 °F) |                 |              |
|---|--------------------------|-----------------|--------------|--------------------------------|-----------------|--------------|
|   | Maximum Stress           | Allowable Limit | Design Ratio | Maximum Stress                 | Allowable Limit | Design Ratio |
| Socket Minimum Cross-Sectional Area       | [[                       |                 |              |                                |                 |              |
| VL Transition Socket to Fin Weld          |                          |                 |              |                                |                 |              |
| VL Fin Minimum Cross-Sectional Area       |                          |                 |              |                                |                 |              |
| Velocity Limiter to Absorber Section Weld |                          |                 |              |                                |                 |              |
| Absorber Section                          |                          |                 |              |                                |                 |              |
| Handle to Absorber Section Weld           |                          |                 |              |                                |                 |              |
| Handle Minimum Cross-Sectional Area       |                          |                 |              |                                |                 | ]]           |

**Table 3-6**  
**C Lattice BWR/4-5 Failed Buffer Scram Stresses**

| Location                                  | Room Temperature (70 °F) |                 |              | Operating Temperature (550 °F) |                 |              |
|---|--------------------------|-----------------|--------------|--------------------------------|-----------------|--------------|
|   | Maximum Stress           | Allowable Limit | Design Ratio | Maximum Stress                 | Allowable Limit | Design Ratio |
| Socket Minimum Cross-Sectional Area       | [[                       |                 |              |                                |                 |              |
| VL Transition Socket to Fin Weld          |                          |                 |              |                                |                 |              |
| VL Fin Minimum Cross-Sectional Area       |                          |                 |              |                                |                 |              |
| Velocity Limiter to Absorber Section Weld |                          |                 |              |                                |                 |              |
| Absorber Section                          |                          |                 |              |                                |                 |              |
| Handle to Absorber Section Weld           |                          |                 |              |                                |                 |              |
| Handle Minimum Cross-Sectional Area       |                          |                 |              |                                |                 | ]]           |

**Table 3-7**  
**S Lattice BWR/6 Failed Buffer Scram Stresses**

| Location                                  | Room Temperature (70 °F) |                 |              | Operating Temperature (550 °F) |                 |              |
|---|--------------------------|-----------------|--------------|--------------------------------|-----------------|--------------|
|   | Maximum Stress           | Allowable Limit | Design Ratio | Maximum Stress                 | Allowable Limit | Design Ratio |
| Socket Minimum Cross-Sectional Area       | [[                       |                 |              |                                |                 |              |
| VL Transition Socket to Fin Weld          |                          |                 |              |                                |                 |              |
| VL Fin Minimum Cross-Sectional Area       |                          |                 |              |                                |                 |              |
| Velocity Limiter to Absorber Section Weld |                          |                 |              |                                |                 |              |
| Absorber Section                          |                          |                 |              |                                |                 |              |
| Handle to Absorber Section Weld           |                          |                 |              |                                |                 |              |
| Handle Minimum Cross-Sectional Area       |                          |                 |              |                                |                 | ]]           |

**Table 3-8**  
**Outer Edge Bending Strain due to Seismic and Channel Bow Bending, Internal Absorber Tube Pressure and Failed Buffer Scram**

| Description  | D Lattice | C Lattice | S Lattice |
|--|-----------|-----------|-----------|
|  | 550 °F    | 550 °F    | 550 °F    |
| Outer Edge Bending Strain, Seismic (%)   | [[        |           |           |
| Outer Edge Bending Strain, Seismic + Channel Bow (%)   |           |           |           |
| Max Internal Pressure Axial Stress (ksi)   |           |           |           |
| Max Failed Buffer Scram Stress (ksi)   |           |           |           |
| Total Outer Edge Strain, Seismic + Failed Buffer Scram + Absorber Tube Internal Pressure (%)               |           |           |           |
| Total Outer Edge Strain, Seismic + Channel Bow + Failed Buffer Scram + Absorber Tube Internal Pressure (%) |           |           |           |
| Allowable Strain (%) ½ Ultimate, Irradiated  |           |           |           |
| Design Ratio   |           |           | ]]        |

**Table 3-9**  
**Absorber Tube to Tie Rod Weld Stress**

| Description  | D Lattice<br>550 °F | C Lattice<br>550 °F | S Lattice<br>550 °F |
|--|---------------------|---------------------|---------------------|
| Seismic + Internal Pressure, Max $S_{INT}$ (ksi)               | [[                  |                     |                     |
| Seismic + Channel Bow + Internal Pressure, Max $S_{INT}$ (ksi) |                     |                     |                     |
| Ultimate Tensile Stress (ksi)                                  |                     |                     |                     |
| Design Ratio   |                     |                     | ]]                  |

**Table 3-10**  
**Stuck Rod Compression Buckling – Entire Control Rod (Mode A)**

| Description                                    | D Lattice |        | C Lattice |        | S Lattice |        |
|--|-----------|--------|-----------|--------|-----------|--------|
|  | 70 °F     | 550 °F | 70 °F     | 550 °F | 70 °F     | 550 °F |
| Critical Buckling Load, $P_{cr}$ (lb)          | [[        |        |           |        |           |        |
| Compressive Yield Load (lb)                    |           |        |           |        |           |        |
| Maximum Stuck Rod Compression Load (lb)        |           |        |           |        |           |        |
| Added Compression Load due to Channel Bow (lb) |           |        |           |        |           |        |
| Total Compressive Load (lb)                    |           |        |           |        |           |        |
| Design Ratio, Buckling                         |           |        |           |        |           |        |
| Design Ratio, Compressive Yield                |           |        |           |        |           | ]]     |

**Table 3-11**  
**Stuck Rod Compression Buckling – Control Rod Wing (Mode B)**

| Description                           | D Lattice |        | C Lattice |        | S Lattice |        |
|---------------------------------------|-----------|--------|-----------|--------|-----------|--------|
|                                       | 70 °F     | 550 °F | 70 °F     | 550 °F | 70 °F     | 550 °F |
| Critical Buckling Load, $P_{cr}$ (lb) | [[        |        |           |        |           |        |
| Compressive Yield Load (lb)           |           |        |           |        |           |        |
| Total Compressive Load (lb)           |           |        |           |        |           |        |
| Design Ratio, Buckling                |           |        |           |        |           |        |
| Design Ratio, Compressive Yield       |           |        |           |        |           | ]]     |

**Table 3-12  
 Boron Carbide Peak Temperatures**

| Parameter                                    | Nominal Dimensions |           | Worst Case Dimensions |           |
|--|--------------------|-----------|-----------------------|-----------|
|  | D/S Lattice        | C Lattice | D/S Lattice           | C Lattice |
| B <sub>4</sub> C Centerline Temperature (°F) | [[                 |           |                       |           |
| Average B <sub>4</sub> C Temperature (°F)    |                    |           |                       |           |
| Helium Release Fraction (%)                  |                    |           |                       | ]]        |

**Table 3-13  
 Handle Lifting Load Stress**

| Lattice Type         | Handle Type           | Maximum Stress Intensity (ksi) | Design Ratio, 1/2 Ultimate Stress |
|----------------------|-----------------------|--------------------------------|-----------------------------------|
| D Lattice<br>BWR/2-4 | BWR/4 Extended Handle | [[                             |                                   |
|                      | BWR/3 Extended Handle |                                |                                   |
|                      | Standard Handle       |                                |                                   |
| C Lattice<br>BWR/4-5 | Extended Handle       |                                |                                   |
|                      | Standard Handle       |                                |                                   |
| S Lattice<br>BWR/6   | Standard Handle       |                                | ]]                                |

**Table 3-14**  
**Fatigue Usage due to Failed Buffer Scram**

| Location                        | D Lattice         |                  |               |       | C Lattice         |                  |               |       | S Lattice         |                  |               |       |
|---------------------------------|-------------------|------------------|---------------|-------|-------------------|------------------|---------------|-------|-------------------|------------------|---------------|-------|
|                                 | Stress Amp. (ksi) | Allow Cycles (N) | Actual Cycles | Usage | Stress Amp. (ksi) | Allow Cycles (N) | Actual Cycles | Usage | Stress Amp. (ksi) | Allow Cycles (N) | Actual Cycles | Usage |
| Transition Piece to Fin Weld    | [[                |                  |               |       |                   |                  |               |       |                   |                  |               |       |
| VL Fin to Absorber Section Weld |                   |                  |               |       |                   |                  |               |       |                   |                  |               | ]]    |

**Table 3-15**  
**Fatigue Usage at Absorber Section Outer Edge**

| Stress Type   | D Lattice         |                  |               |       | C Lattice         |                  |               |       | S Lattice         |                  |               |       |
|---|-------------------|------------------|---------------|-------|-------------------|------------------|---------------|-------|-------------------|------------------|---------------|-------|
|   | Stress Amp. (ksi) | Allow Cycles (N) | Actual Cycles | Usage | Stress Amp. (ksi) | Allow Cycles (N) | Actual Cycles | Usage | Stress Amp. (ksi) | Allow Cycles (N) | Actual Cycles | Usage |
| Absorber Section Outer Edge - Scram + Internal Pressure | [[                |                  |               |       |                   |                  |               |       |                   |                  |               |       |
| Absorber Section Outer Edge – Seismic + Channel Bow     |                   |                  |               |       |                   |                  |               |       |                   |                  |               | ]]    |
|   | Total Usage =     |                  | [[            | ]]    | Total Usage =     |                  | [[            | ]]    | Total Usage =     |                  | [[            | ]]    |

**Table 3-16**  
**Fatigue Usage at Absorber Tube to Tie Rod Weld**

| Stress Type   | D Lattice         |                  |               |       | C Lattice         |                  |               |       | S Lattice         |                  |               |       |
|---|-------------------|------------------|---------------|-------|-------------------|------------------|---------------|-------|-------------------|------------------|---------------|-------|
|   | Stress Amp. (ksi) | Allow Cycles (N) | Actual Cycles | Usage | Stress Amp. (ksi) | Allow Cycles (N) | Actual Cycles | Usage | Stress Amp. (ksi) | Allow Cycles (N) | Actual Cycles | Usage |
| Absorber Tube to Tie Rod Weld - Scram                                     | [[                |                  |               |       |                   |                  |               |       |                   |                  |               |       |
| Absorber Tube to Tie Rod Weld – Seismic + Channel Bow + Internal Pressure |                   |                  |               |       |                   |                  |               |       |                   |                  |               | ]]    |
|   | Total Usage =     |                  | [[            | ]]    | Total Usage =     |                  | [[            | ]]    | Total Usage =     |                  | [[            | ]]    |

**Table 3-17**  
**Hafnium Rod Dimensions**

| Parameter   | D/S Lattice | C Lattice |
|---|-------------|-----------|
| DIA <sub>70</sub> , Maximum Hafnium Rod Diameter (in)                 | [[          |           |
| DIA <sub>550</sub> , Maximum Hafnium Diameter, Thermal Expansion (in) |             |           |
| Minimum Absorber Tube Inside Diameter After Welding (in)              |             | ]]        |

**Table 3-18  
 Irradiated Boron Carbide Capsule Swelling Calculation**

| Parameter  | D/S Lattice | C Lattice |
|--|-------------|-----------|
| Absorber Tube ID Before Welding (in)               | [[          |           |
| <b>Minimum Absorber Tube ID After Welding (in)</b> |             |           |
| Capsule OD (in)                                    |             |           |
| Capsule Wall Thickness (in)                        |             |           |
| Maximum Capsule OD <sub>0</sub> (in)               |             |           |
| Maximum Capsule ID <sub>0</sub> (in)               |             |           |
| Capsule ID strain (in/in)                          |             |           |
| Capsule OD strain (in/in)                          |             |           |
| <b>Capsule OD at 100% local depletion (in)</b>     |             | ]]        |

**Table 3-19  
 Absorber Tube Pressurization Results: Minimum Material Condition with OD and ID Surface Defects**

| Lattice | Temp (°F) | External Pressure (psi) | FEA Burst Pressure (psi) | Allowable Pressure (psi) |
|---------|-----------|-------------------------|--------------------------|--------------------------|
| C       | 70        | 14.7                    | [[                       |                          |
| C       | 550       | 1050                    |                          |                          |
| D       | 70        | 14.7                    |                          |                          |
| D       | 550       | 1050                    |                          | ]]                       |

**Table 3-20**  
**Absorber Tube Pressurization Results: Principle Stress Results at Operating Temperature and Pressure and Maximum Allowable Pressure**

| <b>Stress Component</b> | <b>D/S Lattice</b> | <b>C Lattice</b> |
|-------------------------|--------------------|------------------|
| S1 (Hoop)               | [[                 |                  |
| S2 (Axial)              |                    |                  |
| S3 (Radial)             |                    |                  |
| Stress Intensity        |                    |                  |
| Equivalent Stress       |                    | ]]               |

**Table 3-21**  
**D/S Lattice Burst Pressure Results from FEA and Testing**

| <b>Parameter (D/S Lattice)</b>   | <b>Burst Pressure (psia)</b> |
|--|------------------------------|
| Nominal Dimensions (FEA)   | [[                           |
| Worst-Case Dimensions and Maximum Surface Defects (Design Basis) (FEA) |                              |
| <b>Specimen 1 Tested Burst Pressure</b>                                |                              |
| <b>Specimen 2 Tested Burst Pressure</b>                                | ]]                           |

**Table 3-22**  
**D/S Lattice Thermal Analysis Results**

| Location             | Nodal Temp (°F)    |                       |
|----------------------|--------------------|-----------------------|
|                      | Nominal Dimensions | Worst Case Dimensions |
| Centerline           | [[                 |                       |
| Ring1 OD             |                    |                       |
| Ring2 OD             |                    |                       |
| Ring3 OD             |                    |                       |
| Ring4 OD             |                    |                       |
| Ring5 OD             |                    |                       |
| Ring6 OD             |                    |                       |
| Ring7 OD             |                    |                       |
| Ring8 OD             |                    |                       |
| Capsule ID           |                    |                       |
| Capsule OD           |                    |                       |
| Abs Tube ID          |                    |                       |
| Abs Tube OD          |                    |                       |
| Crud Surface         |                    |                       |
| Avg B <sub>4</sub> C |                    |                       |
| Avg He Void          |                    | ]]                    |

**Table 3-23**  
**C Lattice Thermal Analysis Results**

| Location             | Nodal Temp (°F)    |                    |
|----------------------|--------------------|--------------------|
|                      | Nominal Dimensions | Nominal Dimensions |
| Centerline           | [[                 |                    |
| Ring1 OD             |                    |                    |
| Ring2 OD             |                    |                    |
| Ring3 OD             |                    |                    |
| Ring4 OD             |                    |                    |
| Ring5 OD             |                    |                    |
| Ring6 OD             |                    |                    |
| Ring7 OD             |                    |                    |
| Ring8 OD             |                    |                    |
| Capsule ID           |                    |                    |
| Capsule OD           |                    |                    |
| Abs Tube ID          |                    |                    |
| Abs Tube OD          |                    |                    |
| Crud Surface         |                    |                    |
| Avg B <sub>4</sub> C |                    |                    |
| Avg He Void          |                    | ]]                 |

**Table 3-24**  
**Finite Element Analysis Summary**

| Analysis Description   | Section | Geometry Inputs   | Applied Loads  | Material Properties   | Acceptance Criteria  | Marathon-Ultra Comparison to Marathon-5S  |
|--|---------|---|--|---|--|---|
| <u>Thermal Analysis</u> : Determines the temperature of boron carbide during operation. Uses heat generation due to neutron capture.   | 3.6.3   | Absorber tube and capsule geometries. Worst-case geometries (largest helium gap) are used. Internal wing absorber tube modeled by assuming zero heat flux to adjacent tubes. Conservative crud build-up used. | Peak boron carbide heat generation rates from nuclear analyses.  | Thermal conductivities from various sources.  | Thermal stress less than allowable stress.   | Identical methodology. Only difference is incorporating Marathon-Ultra capsule geometry and heat generation rates.  |
| <u>Lifting Load</u> : Determines stresses in the handle while lifting the control rod.   | 3.7     | Worst-case geometry from handle drawings.   | 2x control rod weight  | Unirradiated linear-elastic material properties.  | Maximum stress intensity is compared to material allowable stress.   | Identical methodology. Only difference is slightly heavier Marathon-Ultra weights, resulting in slightly larger loads. Analysis shows linear relationship between control rod weight and peak stress intensity. |
| <u>External Pressure + Channel Bow Lateral Load</u> : Determines stresses in the absorber tube due to lateral loads imposed by bowed fuel channels combined with RPV operating pressure. | 3.4.3   | One-quarter affected tube with ¼-symmetry boundary conditions. Worst-case dimensions.   | Maximum lateral loads from fuel channel bow studies.   | Unirradiated linear-elastic material properties. Also checked using unirradiated elastic-plastic true stress-strain curves. | Maximum stress intensity compared to material allowable stress.  | Identical   |
| <u>Internal Pressure</u> : Determines maximum allowable absorber tube internal pressure.   | 3.6.4   | Uses worst-case tube dimensions and allowable surface defects. Also checked first tube attached to the tie rod (tie rod modeled as an empty tube).  | Reactor pressure vessel internal pressure to exterior of tubes for 'hot' cases. Unirradiated property analyses determine maximum allowable internal pressure. 'Check' analyses apply this pressure as appropriate. | Unirradiated elastic-plastic true stress-strain curves. Also checked using irradiated material properties.                  | Burst pressure defined to be internal pressure at which the stress intensity at any location in the tube first reaches the true ultimate strength. Then, a factor of safety of 2.0 is used to determine an allowable pressure. | Identical   |
| <u>Pressurization Stress on Absorber Tubes</u> : Finite element analysis is used to determine the radial, hoop, and axial stress in the absorber tube at allowable internal pressure.    | 3.6.4   | Worst-case absorber tube dimensions.  | Maximum allowable pressure determined in internal pressure analysis.   | Unirradiated elastic-plastic true stress-strain curves.   | Combined stresses less than material allowable stresses.   | Identical   |
| <u>Combined Internal Pressure + Fuel Channel Bow Induced Bending</u> : Determines maximum stresses in the absorber tube to tie rod weld.   | 3.4.2   | Worst-case absorber tube dimensions. Model consists of tie rod and entire wing of absorber tubes.   | Lateral loads from channel bow studies and seismic event limits.   | Unirradiated elastic-plastic true stress-strain curves.   | Maximum stress intensity less than material allowable stress.  | Identical   |

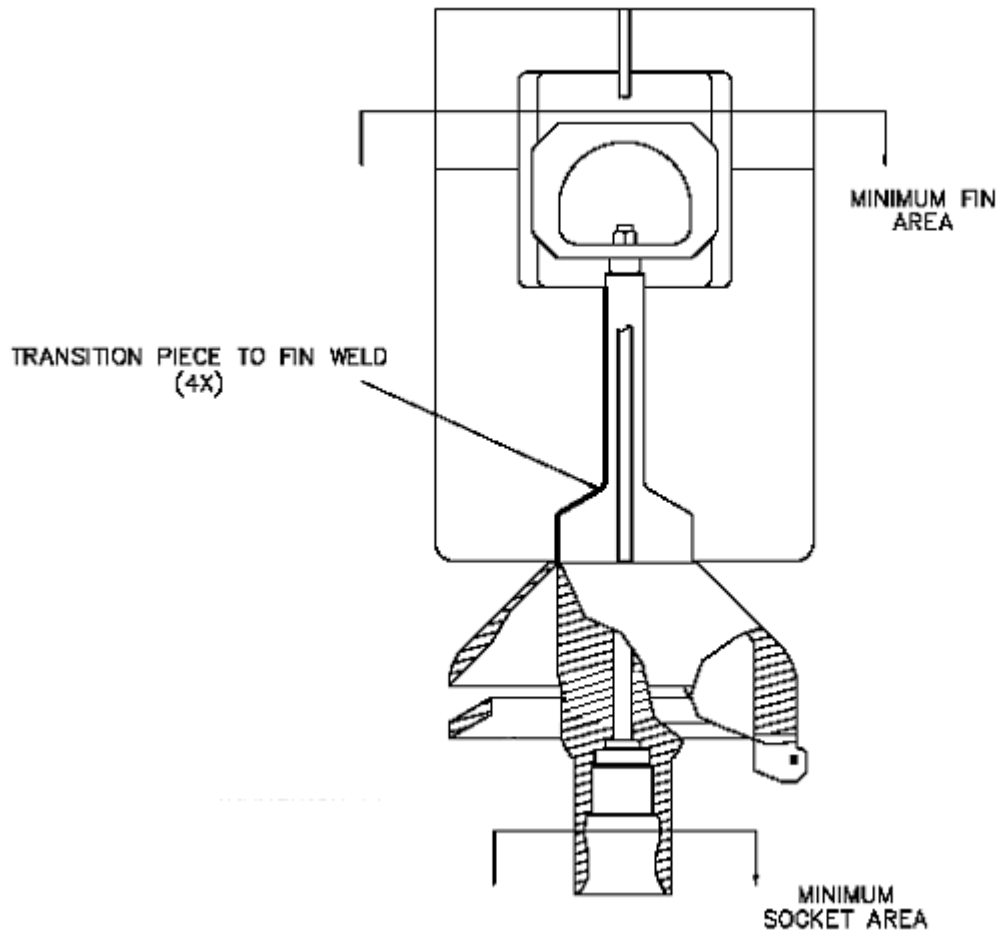


**Figure 3-1. Velocity Limiter Welds and Cross-Sections Analyzed**

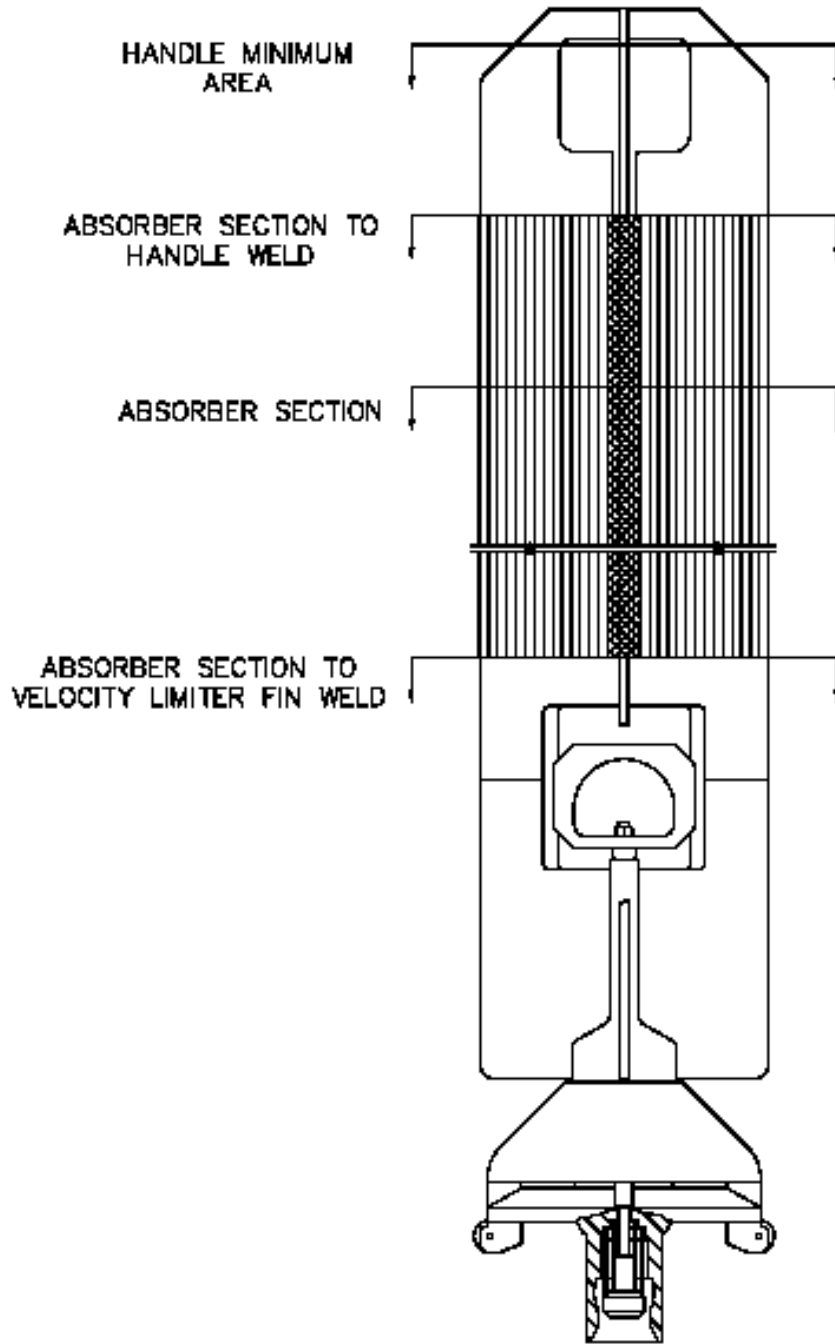


**Figure 3-2. Control Rod Assembly Welds and Cross-Sections Analyzed**

[[ ]]

**Figure 3-3. Absorber Tube to Tie Rod Finite Element Model**

[[ ]]

**Figure 3-4. Lateral Load Finite Element Model**

[[ ]]

**Figure 3-5. Lateral Load Finite Element Results (C Lattice)**

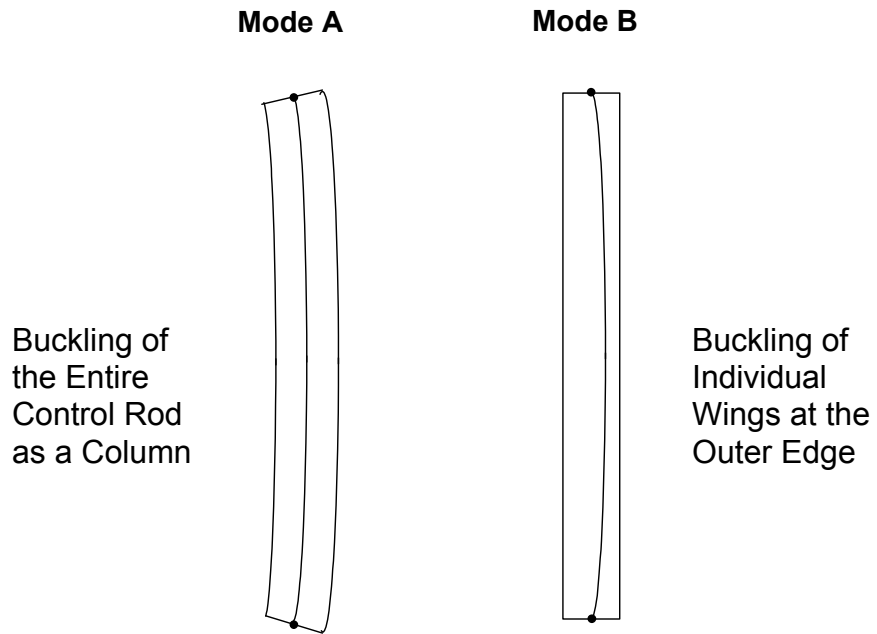


**Figure 3-6. Control Rod Buckling Modes**

[[ ]]

**Figure 3-7. Absorber Tube Pressurization Finite Element Model**

[[ ]]

**Figure 3-8. Absorber Tube and Capsule Thermal Finite Element Model**

[[

]]

**Figure 3-9. Handle Lifting Loads Finite Element Model**

[[

]]

**Figure 3-10. D/S Lattice Thermal Analysis Results**

[[

]]

**Figure 3-11. C Lattice Thermal Analysis Results**

[[ ]]

**Figure 3-12. Stress Intensity Distribution for Multiple Tube Pressurization Finite Element Model, All Tubes Pressurized**

[[

]]

**Figure 3-13. Absorber Tube Burst Pressure Test Specimen – After Test**

[[

]]

**Figure 3-14. Absorber Tube Burst Pressure Test Specimen Rupture**

[[

]]

**Figure 3-15. Irradiated Boron Carbide Diametral Swelling Data**

[[

]]

**Figure 3-16. Irradiated Hafnium Diameter Data**

## 4. NUCLEAR EVALUATIONS

### 4.1 DESIGN CRITERIA

A control rod's nuclear worth characteristics shall be compatible with reactor operation requirements. As approved in References 1 and 2, a replacement control rod can meet these requirements by demonstrating that the initial hot and cold CRB reactivity worths are within  $\pm 5\%$   $\Delta k/k$  (where  $\Delta k/k$  is  $1-k_{con}/k_{unc}$ ) of the original equipment control rod blade design worth. Replacement rods with reactivity worth outside this tolerance require, as a minimum, evaluations on cold shutdown margin, AOO CPR, control rod drop accident, fuel cycle economics, nuclear methods, and control rod lifetime.

For GEH original equipment control rods, the nuclear lifetime is defined as the quarter-segment depletion at which the control rod cold worth ( $\Delta k/k$ ) is 10% less than its zero-depletion cold worth. The original equipment (DuraLife 100) control rods consist of thin sheaths enclosing boron carbide filled tubes. The sheaths are welded to a central tie rod to form the cruciform shape of the control rods. The original equipment control rods are shown in Figure 4-7.

As discussed above, a retrofit design may have an initial cold worth that differs from the original equipment control rod that it is replacing, within  $\pm 5\%$  of the initial worth of that control rod (the "matched worth" criterion). The nuclear lifetime for such a retrofit control rod is defined as the quarter-segment depletion at which the cold worth is the same as the end-of-nuclear-life cold worth of the original equipment control rod that it is replacing.

### 4.2 METHODOLOGY

The methodology applied to the Marathon-Ultra control rod is identical to the methodology of the Marathon-5S analysis approved in Reference 1. This includes the use of the same computer codes, described below, and in the Reference 1 report.

The nuclear lifetime for a particular control blade design is determined with a two-dimensional step-wise depletion of the control blade poisons. This is done by computing the eigenvalue for hot, voided conditions with a Monte Carlo neutron transport code. The poison reaction rates from the analysis are then assumed to be constant for a fixed period of time ( $\Delta t$ ) to obtain the number of absorptions for each discrete area of the blade. The poison number densities are then updated in the Monte Carlo code input and another eigenvalue calculation is performed. This process continues until the reduction in cold worth – as computed by companion cold Monte Carlo eigenvalue calculations – reaches the end-of-nuclear-life criterion.

For locations within the blade that use boron carbide as a poison, the change in the number of absorber atoms is computed as:

$$\frac{dN_{B-10}}{dt} = - (N \cdot \sigma)_{B-10}$$

Here,  $\sigma$  is the reaction rate for B-10 from the Monte Carlo code.

The number of absorptions from each of the regions is summed to obtain the total number of absorptions (A) for the time interval. This total number of absorptions is normalized by the total number of B-10 atoms if the design would have incorporated only boron carbide as an absorber. The resulting value is the B-10 equivalent depletion:

$$\%_{\text{depletion}} = \frac{A}{N_{\text{B-10}}}$$

Reactivity worth calculations for the Marathon-5S are performed using a GEH controlled version of MCNP4A, which was developed by the Los Alamos National Laboratory (Reference 3). MCNP is a Monte Carlo code for solving the neutral-particle transport equation as a fixed source or an eigenvalue problem in three dimensions. Continuous energy cross-section data is used in the calculation, thus making creation of multi-group cross-sections unnecessary. The use of MCNP is the only process change from the original Marathon nuclear analysis, which used MERIT. Otherwise, depletion calculations remain unchanged.

Two additional utility codes are used in conjunction with MCNP. The GEH utility code "MODL" is used to set up the MCNP input deck, based on lattice design data and control rod design data. The GEH utility code "HO" is coupled to MCNP for the depletion calculation. It reads the MCNP tallies (cell fluxes and absorber cross-sections) and then performs the control blade depletion calculation. The depleted absorber atom densities are then used to update the MCNP inputs for the next time step. MCNP input data for cold case are also generated with "HO" by modifying the input data from the hot inputs.

For the depletion calculations that are performed for each fuel lattice, the time step used is 100 days. In order to reach the 10% cold worth reduction for the nuclear lifetime evaluation, a total of 21 time steps are used for the re-calculation of DuraLife 100 (original equipment), and a total of 30 time steps are used for the calculation of Marathon-Ultra lifetime. Tables 4-13 through 4-15 contain input parameters used to model the original equipment and Marathon-Ultra control rods.

The self-shielding characteristics of B-10, defined as the faster depletion of B-10 on the outer edge of B<sub>4</sub>C column than the average pin due to spatial self-shielding of B-10, is accounted for in the MCNP calculations. The calculations use a ring model that divides each B<sub>4</sub>C column into four concentric rings of equal cross-sectional area. The radii of the boron carbide rings used in the updated analysis are shown in Table 4-12.

### 4.3 CONTROL ROD NUCLEAR LIFETIME

A description of the fuel bundles used for the D, C, and S lattice control rod nuclear lifetime calculations are shown in Figures 4-1 through 4-3. Both the hot and cold calculation results for the peak ¼ segment are shown in Tables 4-1 through 4-3. The cold calculation results, on which the nuclear lifetime is based, are shown graphically in Figures 4-4 through 4-6. The nuclear lifetimes, based on a cold worth equal to a cold worth reduction of 10% for an original equipment control rod are summarized in Table 4-4.

#### 4.4 INITIAL CONTROL ROD WORTH

As discussed above, a control rod with an initial (non-depleted) reactivity worth within  $\pm 5\%$  of the original equipment control rod is considered “matched worth” and therefore, does not require any special treatment in plant core analyses. The initial cold and hot worths (0% depletion) of the Marathon-Ultra control rod designs are found in Tables 4-1 through 4-3. These values of  $\Delta k/k$  are then compared to the worths of the original equipment control rods in Tables 4-6 through 4-8. All cold and hot initial control rod worths are within  $\pm 5\%$  of the original equipment, and can be considered to be direct nuclear replacements of the original equipment.

#### 4.5 HEAT GENERATION RATES

The capture of neutrons by B-10 atoms results in the release of energy, or heat generation. As discussed in Section 3.6, a thermal model of the absorber tube and capsule is used to calculate boron carbide temperatures within the capsules, which affects the rate of helium release. The heat generation rates for the Marathon-Ultra designs are calculated assuming 2.79 MeV per neutron capture in B-10. Then, a radial peaking factor is employed to determine the heat generation rate in the highest fluence absorber tube, which is the outermost tube.

Both average and peak heat generation rates are shown in Table 4-5. The peak heat generation rates are used in the thermal model discussed in Section 3.6 to determine the capsule boron carbide temperatures shown in Table 3-12.

#### 4.6 CONTROL ROD MECHANICAL LIFETIME

The control rod mechanical lifetime methodology is identical to the Marathon-5S methodology approved in Reference 1. As discussed in Section 3.6, the lifetime limiting mechanism for the Marathon-Ultra control rod is the pressurization of the absorber tubes due to the helium release from the irradiated boron carbide. An absorber tube mechanical limit as a function of average B-10 per cent depletion is calculated based on peak heat generation, temperatures and helium release fractions, combined with worst-case component geometries. As discussed in Section 3.6, the method for evaluating the swelling phenomenon of irradiated boron carbide is very conservative, using worst-case capsule and absorber tube dimensions, along with a  $+3\sigma$  upper limit swelling rate assumption. Using these conservatisms, the Marathon-Ultra capsule is designed [[

]]

The table used to calculate the control rod mechanical lifetime limit, in terms of a four-segment average B-10 depletion, is shown in Tables 4-9, 4-10 and 4-11 for D, C, and S lattice applications. Along the top of the table is the absorber tube number, where tube 1 is the first absorber tube, welded to the cruciform tie rod. Also shown are the span-wise radial peaking factors, which show the relative absorption rate of each absorber tube. A limiting axial depletion profile is used to calculate the B-10 depletion for each absorber tube and axial node. At the bottom of the table, the average depletion for each tube is shown, along with the depletion limit for that tube, which varies depending on the number of empty capsule plenums employed at the bottom of the absorber column. Through an iterative process, the peak  $\frac{1}{4}$  segment depletion is raised until the limiting absorber tube reaches its mechanical limit. The 4-segment mechanical

NEDO-33284 Supplement 1 Revision 0  
Non-Proprietary Information

lifetime of the control rod is then the average of the four  $\frac{1}{4}$  segments. The 4 segment mechanical lifetime limits are summarized in Table 4-4, along with the peak  $\frac{1}{4}$  segment nuclear lifetime limits.

Tables 4-9 through 4-11 calculate the average depletion in all absorber tubes, at nuclear end of life. To accomplish this, the  $\frac{1}{4}$ -segment nuclear limit is entered into the peak  $\frac{1}{4}$ -segment. As shown along the bottom of the tables, the average depletion for each tubes is well below each tubes' limit. Therefore, the nuclear lifetime of the Marathon-Ultra control rod is limiting, in that the mechanical lifetime exceeds the nuclear lifetime for all cases.

**Table 4-1**  
**D Lattice Depletion Calculation Results**

| Irradiation Time (days) | Equivalent B-10 Depletion (%) | Hot, Voided Eigenvalue | Hot Worth ( $\Delta k/k$ ) | Hot Change in Worth (%) | Cold Eigenvalue | Cold Worth ( $\Delta k/k$ ) | Cold Change in Worth (%) |
|-------------------------|-------------------------------|------------------------|----------------------------|-------------------------|-----------------|-----------------------------|--------------------------|
| [[                      |                               |                        |                            |                         |                 |                             | ]]                       |

**Table 4-2**  
**C Lattice Depletion Calculation Results**

| Irradiation Time (days) | Equivalent B-10 Depletion (%) | Hot, Voided Eigenvalue | Hot Worth ( $\Delta k/k$ ) | Hot Change in Worth (%) | Cold Eigenvalue | Cold Worth ( $\Delta k/k$ ) | Cold Change in Worth (%) |
|-------------------------|-------------------------------|------------------------|----------------------------|-------------------------|-----------------|-----------------------------|--------------------------|
| []                      |                               |                        |                            |                         |                 |                             | []                       |

**Table 4-3**  
**S Lattice Depletion Calculation Results**

| Irradiation Time (days) | Equivalent B-10 Depletion (%) | Hot, Voided Eigenvalue | Hot Worth ( $\Delta k/k$ ) | Hot Change in Worth (%) | Cold Eigenvalue | Cold Worth ( $\Delta k/k$ ) | Cold Change in Worth (%) |
|-------------------------|-------------------------------|------------------------|----------------------------|-------------------------|-----------------|-----------------------------|--------------------------|
| [[                      |                               |                        |                            |                         |                 |                             | ]]                       |

**Table 4-4  
 Marathon-Ultra Control Rod Nuclear and Mechanical Depletion Limits**

| <b>Application</b> | <b>End of Life B-10 Equivalent Depletion (%)</b> |  |
|--------------------|--|--|
|                    | <b>Nuclear<br/>Peak Quarter Segment</b>          | <b>Mechanical<br/>Four Segment Average</b> |
| D Lattice, BWR/2-4 | [[   |  |
| C Lattice, BWR/4,5 |  |  |
| S Lattice, BWR/6   |  | ]]   |

**Table 4-5  
 Heat Generation Rates**

| <b>Application</b> | <b>Average Heat<br/>Generation Rate<br/>(Watts/gram B<sub>4</sub>C)</b> | <b>Radial Peaking<br/>Factor</b> | <b>Peak Tube Heat<br/>Generation Rate<br/>(Watts/gram B<sub>4</sub>C)</b> |
|--------------------|---|----------------------------------|---|
| D Lattice, BWR/2-4 | [[  |                                  |   |
| C Lattice, BWR/4,5 |   |                                  |   |
| S Lattice, BWR/6   |   |                                  | ]]  |

**Table 4-6**  
**Initial Reactivity Worth, D Lattice (BWR/2-4) Original Equipment and Marathon-Ultra CRBs**

| <b>Condition</b> | <b>Original Equipment <math>\Delta k/k</math></b> | <b>Marathon-Ultra <math>\Delta k/k</math></b> | <b>Marathon-Ultra Change from Original Equipment</b> |
|------------------|---|---|--|
| Cold             | [[  |   |  |
| Hot (40% Void)   |   |   | ]]   |

**Table 4-7**  
**Initial Reactivity Worth, C Lattice (BWR/4,5) Original Equipment and Marathon-Ultra CRBs**

| <b>Condition</b> | <b>Original Equipment <math>\Delta k/k</math></b> | <b>Marathon-Ultra <math>\Delta k/k</math></b> | <b>Marathon-Ultra Change from Original Equipment</b> |
|------------------|---|---|--|
| Cold             | [[  |   |  |
| Hot (40% Void)   |   |   | ]]   |

**Table 4-8**  
**Initial Reactivity Worth, S Lattice (BWR/6) Original Equipment and Marathon-Ultra CRBs**

| <b>Condition</b> | <b>Original Equipment <math>\Delta k/k</math></b> | <b>Marathon-Ultra <math>\Delta k/k</math></b> | <b>Marathon-Ultra Change from Original Equipment</b> |
|------------------|---|---|--|
| Cold             | [[  |   |  |
| Hot (40% Void)   |   |   | ]]   |

**Table 4-9**  
**D Lattice Mechanical Lifetime Calculation**

[[

]]

**Table 4-10**  
**C Lattice Mechanical Lifetime Calculation**

[[

]]

**Table 4-11**  
**S Lattice Mechanical Lifetime Calculation**

[[

]]

**Table 4-12**  
**Boron Carbide Ring Radii in MCNP Model**

| Ring Number | Ring Radial Thickness (cm)         |                              |
|-------------|------------------------------------|------------------------------|
|             | Marathon-Ultra,<br>D and S Lattice | Marathon-Ultra,<br>C Lattice |
| 1 (inner)   | [[                                 |                              |
| 2           |                                    |                              |
| 3           |                                    |                              |
| 4 (outer)   |                                    | ]]                           |

**Table 4-13**  
**D Lattice Original Equipment and Marathon-Ultra Dimensions**

| Description                                 |        | DuraLife 100 D |      | Marathon-Ultra D |      |
|---|--------|----------------|------|------------------|------|
|   |        | (inches)       | (cm) | (inches)         | (cm) |
| Span  |        | [[             |      |                  |      |
| Half Span                                   | SBL    |                |      |                  |      |
| Wing Thickness (Square Tube Width)          |        |                |      |                  |      |
| Half Wing Thickness                         | TBL    |                |      |                  |      |
| Tie Rod Half Thickness                      | TTR    |                |      |                  |      |
| Radius of Central Support Filet             | RBLF   |                |      |                  |      |
| Radius of Blade Tip                         | RBLT   |                |      |                  |      |
| Span of Central Support (Tie Rod)           |        |                |      |                  |      |
| Half Span of Central Support                | SCS    |                |      |                  |      |
| Thickness of Sheath                         | TSH    |                |      |                  |      |
| Inner Diameter of Tube (Capsule)            | TID    |                |      |                  |      |
| Outer Diameter of Tube                      | TOD    |                |      |                  |      |
| Wall Thickness of Tube                      |        |                |      |                  |      |
| Diameter of Hafnium Rod                     |        |                |      |                  |      |
| Type  | IBLADE |                |      |                  |      |
| Number of B <sub>4</sub> C Tubes (Capsules) | NOPT   |                |      |                  |      |
| Number of Hafnium Rods                      | NOHFT  |                |      |                  |      |
| Number of Empty Tubes                       | NOBT   |                |      |                  | ]]   |

**Table 4-14**  
**C Lattice Original Equipment and Marathon-Ultra Dimensions**

| Description                         |        | DuraLife 100 C |      | Marathon-Ultra C |      |
|-------------------------------------|--------|----------------|------|------------------|------|
|                                     |        | (inches)       | (cm) | (inches)         | (cm) |
| Span                                |        | [[             |      |                  |      |
| Half Span                           | SBL    |                |      |                  |      |
| Blade Thickness (Square Tube Width) |        |                |      |                  |      |
| Half Blade Thickness                | TBL    |                |      |                  |      |
| Tie Rod Half Thickness              | TTR    |                |      |                  |      |
| Radius of Central Support Filet     | RBLF   |                |      |                  |      |
| Radius of Blade Tip                 | RBLT   |                |      |                  |      |
| Span of Central Support (Tie Rod)   |        |                |      |                  |      |
| Half Span of Central Support        | SCS    |                |      |                  |      |
| Thickness of Sheath                 | TSH    |                |      |                  |      |
| Inner Diameter of Tube (Capsule)    | TID    |                |      |                  |      |
| Outer Diameter of Tube              | TOD    |                |      |                  |      |
| Wall Thickness of Tube              |        |                |      |                  |      |
| Diameter of Hafnium Rod             |        |                |      |                  |      |
| Type                                | IBLADE |                |      |                  |      |
| Number of B4C Tubes (Capsules)      | NOPT   |                |      |                  |      |
| Number of Hafnium Rods              | NOHFT  |                |      |                  |      |
| Number of Empty Tubes               | NOBT   |                |      |                  | ]]   |

**Table 4-15**  
**S Lattice Original Equipment and Marathon-Ultra Dimensions**

| Description                        |        | DuraLife 100 S |      | Marathon-Ultra S |      |
|------------------------------------|--------|----------------|------|------------------|------|
|                                    |        | (inches)       | (cm) | (inches)         | (cm) |
| Span                               |        | [[             |      |                  |      |
| Half Span                          | SBL    |                |      |                  |      |
| Wing Thickness (Square Tube Width) |        |                |      |                  |      |
| Half Wing Thickness                | TBL    |                |      |                  |      |
| Tie Rod Half Thickness             | TTR    |                |      |                  |      |
| Radius of Central Support Filet    | RBLF   |                |      |                  |      |
| Radius of Blade Tip                | RBLT   |                |      |                  |      |
| Span of Central Support (Tie Rod)  |        |                |      |                  |      |
| Half Span of Central Support       | SCS    |                |      |                  |      |
| Thickness of Sheath                | TSH    |                |      |                  |      |
| Inner Diameter of Tube (Capsule)   | TID    |                |      |                  |      |
| Outer Diameter of Tube             | TOD    |                |      |                  |      |
| Wall Thickness of Tube             |        |                |      |                  |      |
| Diameter of Hafnium Rod            |        |                |      |                  |      |
| Type                               | IBLADE |                |      |                  |      |
| Number of B4C Tubes (Capsules)     | NOPT   |                |      |                  |      |
| Number of Hafnium Rods             | NOHFT  |                |      |                  |      |
| Number of Empty Tubes              | NOBT   |                |      |                  | ]]   |

[[

]]

**Figure 4-1. D Lattice Fuel Bundle Rod Position and Enrichment**

[[

]]

**Figure 4-2. C Lattice Fuel Bundle Rod Position and Enrichment**

[[

]]

**Figure 4-3. S Lattice Fuel Bundle Rod Position and Enrichment**

[[

]]

**Figure 4-4. D Lattice Control Rod Cold Worth Reduction with Average Depletion**

[[

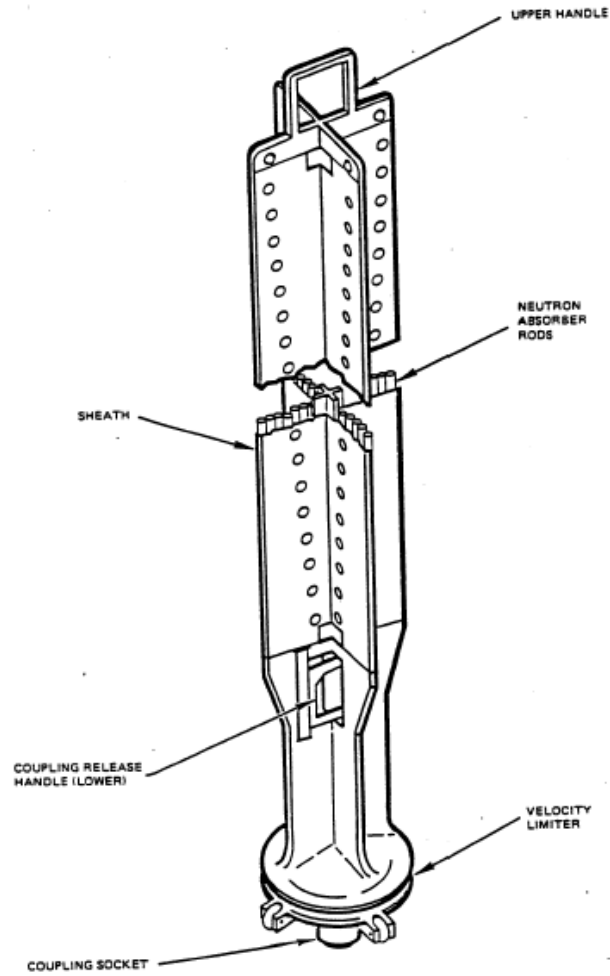
]]

**Figure 4-5. C Lattice Control Rod Cold Worth Reduction with Average Depletion**

[[

]]

**Figure 4-6. S Lattice Control Rod Cold Worth Reduction with Average Depletion**



ORIGINAL EQUIPMENT CONTROL ROD DESIGN

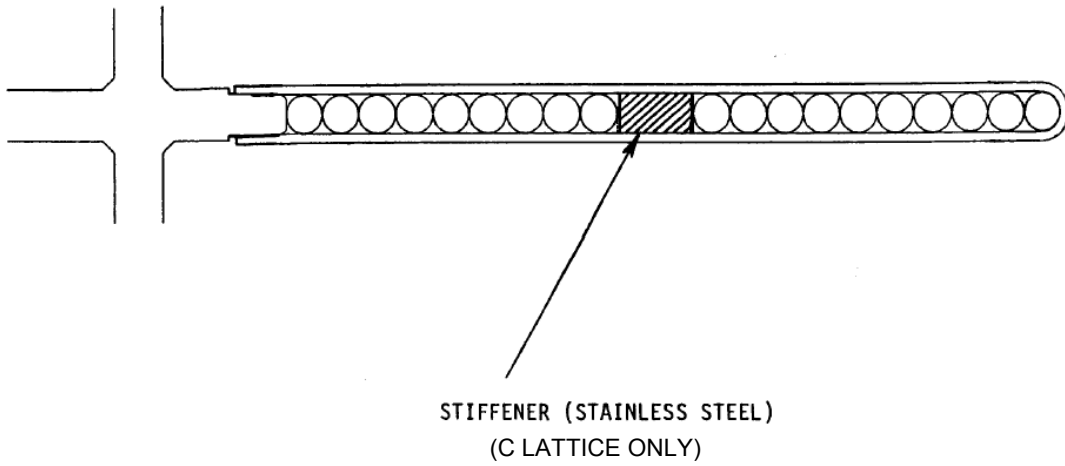


Figure 4-7. BWR/2-6 Original Equipment

## **5. OPERATIONAL EVALUATIONS**

### **5.1 DIMENSIONAL COMPATIBILITY**

As discussed in Section 2, the outer structure of the Marathon-Ultra is identical to the Marathon-5S approved in Reference 1. The width of the absorber tube and the width of the control rod wing of the Marathon-Ultra control rod are also identical to the original Marathon control rod. Plus, all other envelope dimensions, including tie rod, handle, and velocity limiter are identical. Therefore, the fit and clearance of the Marathon-Ultra control rods in the fuel cell is identical to the Marathon and Marathon-5S control rods.

Reference 10 provides a summary of the inspection history of the Marathon control rod. For all of these inspections, no issues have been identified with respect to the lack of dimensional stability of the Marathon control rod assembly. The inspections have not shown signs of excessive wear on the control rod due to any distortion of the control rod assembly.

Therefore, the inspection history of the Marathon control rod demonstrates that the Marathon design is dimensionally stable, even with significant amounts of irradiation and residence time.

### **5.2 SCRAM TIMES**

An OBE or SSE earthquake condition could cause the fuel channels to temporarily bow or bend. In addition, as fuel channels age, they tend to both bulge and bow, which can negatively affect the insertion capability of the control rod blade.

Previous Marathon prototype scram testing shows that the insertion capability of the CRB is affected by the stiffness of the assembly. The stiffer (less flexible) the control rod assembly, the longer the scram times. The stiffness of the Marathon-5S and Marathon-Ultra control rods have been evaluated to be equal to or less stiff than the Marathon CRB, in terms of the assembly cross-sectional area moment of inertia. Therefore, the Marathon-Ultra control rod will have a scram insertion capability equal to or better than the Marathon CRB, in the event of temporary or permanent channel deformation.

The overall assembly weight of the Marathon-Ultra CRB is not greater than the maximum weights of Marathon control rod designs produced. This, combined with the bending stiffness characteristics, ensure that the Marathon-Ultra CRB design will not have an adverse effect on scram times.

The results of seismic scram tests applicable to the Marathon-Ultra design are discussed in Section 3.4.4. As discussed, for all lattice types, the control rods met the acceptance criteria of successful insertion within scram time requirements under OBE fuel channel deflection conditions, and successful insertion under SSE fuel channel deflection conditions.

### **5.3 'NO SETTLE' CHARACTERISTICS**

A 'no settle' condition may occur in the event of excessive friction between the control rod and the fuel channels. If this additional friction does not allow the weight of the CRB to settle the assembly into a control rod drive (CRD) positional notch, a 'no settle' condition occurs. As

previously discussed, the envelope dimensions for the Marathon-Ultra CRB are identical to the Marathon and Marathon-5S control rods. Further, the wet (buoyant) weight of the Marathon-Ultra assembly is within the range of weights of previous Marathon and Marathon-5S control rod designs. Therefore, the ability of the Marathon-Ultra assembly to settle into a CRD notch is equal to that of the Marathon or Marathon-5S control rod.

#### 5.4 DROP SPEEDS

The parameters that affect the drop speed of the control rod in the event of a rod drop accident are the weight of the control rod assembly, and the geometry of the “bell” of the velocity limiter. The Marathon-Ultra control rod uses the same cast or FabriCast (hybrid cast/fabricated) velocity limiters as those on the Duralife, Marathon and Marathon-5S control rods. Since the weight of the Marathon-Ultra control rod is less than the weight of the Duralife control rods used for the original drop tests, the Marathon-Ultra control rod will have drop speeds less than the [[ ]] required. Therefore, the Marathon-Ultra CRB will limit the reactivity insertion rate during a CRDA within the existing safety analysis parameters.

#### 5.5 FUEL CELL THERMAL HYDRAULICS

The surface geometry of the Marathon-Ultra and Marathon-5S control rods are different than the Marathon control rod due to the different outer absorber tube geometry. In order to evaluate the effect on the thermal hydraulics of the fuel cell, the total displaced volume of the Marathon-Ultra or Marathon-5S control rod is compared to the Marathon control rod, approved in Reference 1. The S lattice, BWR/6 version of these control rods are chosen for this comparison.

The total displaced volume for the Marathon control rod is [[ ]] the total displaced volume of the Marathon-Ultra control rod is [[ ]], for a difference of [[ ]] from the Marathon control rod. This small difference is judged to be negligible in its effect on the thermal hydraulics of the fuel cell.

The topographic differences between the Marathon-Ultra and the Marathon control rods is less significant than the differences between the Marathon control rods and DuraLife type control rods and control rods from other vendors. These small topographic changes will have no significant effect on the thermal hydraulics of the fuel cell.

## **6. LICENSING CRITERIA**

The NRC Safety Evaluation Report for the Marathon and Marathon-5S Control Rod Blades (within References 1 and 2) identify five criteria for the licensing and evaluation of BWR control rods. These same five criteria are used for the Marathon-Ultra control rod.

### **6.1 STRESS, STRAIN, AND FATIGUE**

#### **6.1.1 Criteria**

The control rod stresses, strains, and cumulative fatigue shall be evaluated to not exceed the ultimate stress or strain of the material.

#### **6.1.2 Conformance**

As discussed in Section 3, the design changes for the Marathon-Ultra CRB have been evaluated using the same or more conservative design bases and methodology than the Marathon and Marathon-5S control rods. All components of the Marathon-Ultra control rod are found to be acceptable when analyzed for stresses due to normal, abnormal, emergency, and faulted loads. The design ratio, which is the effective stress divided by the stress limit or the effective strain divided by the strain limit, is found to be less than or equal to 1.0 for all components. Conservatism is included in the evaluation by limiting stresses for all primary loads to one-half of the ultimate strength (i.e., a safety factor of two is employed).

The fatigue usage of the Marathon-Ultra control rod is calculated using the same methodology as the Marathon and Marathon-5S control rods. The fatigue analysis assumes [[ ]]. It is found that the calculated fatigue usage is less than the material fatigue capability (the fatigue usage factor is much less than 1.0).

### **6.2 CONTROL ROD INSERTION**

#### **6.2.1 Criteria**

The control rod shall be evaluated to be capable of insertion into the core during all modes of plant operation within the limits assumed in the plant analyses.

#### **6.2.2 Conformance**

The thickness of the wing of the Marathon-Ultra CRB, [[ ]], is identical to the Marathon and Marathon-5S control rods. Other envelope dimensions, including those for control rods with plain handles or with spacer pads, are also identical. Therefore, the fit and clearance of the Marathon-Ultra control rod in the fuel cell is identical to the Marathon and Marathon-5S control rods.

An OBE or SSE earthquake condition potentially could cause the fuel channels to temporarily bow or bend. In addition, as fuel channels age, they tend to both bulge and bow, which can negatively affect the insertion capability of the control rod blade.

Previous Duralife and Marathon prototype seismic scram testing has shown that the insertion capability of the CRB is affected by the stiffness of the assembly and by the assembly weight. If the control rod assembly is stiffer (less flexible), then the scram times are longer. The stiffness of the Marathon-5S and Marathon-Ultra control rods has been evaluated to be equal to or less stiff than the Marathon control rod, in terms of the assembly cross-sectional area moment of inertia. This, combined with the fact that the Marathon-Ultra assembly is lighter than previous control rod designs shows that the Marathon-Ultra CRB has a scram insertion capability equal to or better than the Marathon CRB in the event of temporary or permanent channel deformation.

The results of seismic scram tests, applicable to Marathon-Ultra control rods, are discussed in Section 3.4.4. As discussed, for all lattice types, the control rods successfully inserted within scram time requirements under OBE fuel channel deflection conditions, and successfully inserted under SSE fuel channel deflection conditions. This meets all acceptance criteria for the test.

### **6.3 CONTROL ROD MATERIAL**

#### **6.3.1 Criteria**

The material of the control rod shall be shown to be compatible with the reactor environment.

#### **6.3.2 Conformance**

The Marathon-Ultra CRB uses the same materials as the Marathon and Marathon-5S control rods. No new material has been introduced. The new design absorber tubes are made from the same high purity stabilized type 304 stainless steel (Radiation Resist 304S) as the Marathon absorber tubes. Material testing and the service history of the Marathon control rod blades confirm the resistance to IASCC.

### **6.4 REACTIVITY**

#### **6.4.1 Criteria**

The reactivity worth of the control rod shall be included in the plant core analyses.

#### **6.4.2 Conformance**

The compatibility of the Marathon-Ultra control rod is evaluated using the matched worth criterion approved in the Marathon control rod LTR (Reference 2); that is, replacement control rods whose initial reactivity worth is  $\pm 5\% \Delta k/k$  with respect to the original equipment do not need special treatment in plant core analyses. The nuclear design of the Marathon-Ultra control rod meets this criterion as discussed in Section 4. Therefore, Marathon-Ultra control rods can be used without change to current GEH lattice physics codes and design procedures.

## 6.5 SURVEILLANCE

### 6.5.1 Criteria

Prior to the use of new design features on a production basis, lead surveillance control rods may be used.

### 6.5.2 Conformance

Section 3.3 of Reference 1 Safety Evaluation requires a visual inspection program for the Marathon-5S control rod. The visual inspection program is designed to detect both (1) early-in-life failure mechanisms such as stress corrosion cracking and weld degradation, and (2) end-of-mechanical life predictions such as absorber tube failure. Since the outer structure of the Marathon-Ultra control rod is identical to the Marathon-5S, visual inspections performed for Marathon-5S apply equally to the Marathon-Ultra, satisfying the early-in-life inspection requirements. However, since the Marathon-Ultra has a longer nuclear lifetime than the Marathon-5S, the stainless steel structure of the Marathon-Ultra will achieve a higher irradiation at end of life than the Marathon-5S. Therefore, only an end-of-life surveillance should be required.

A comparison of  $\frac{1}{4}$ -segment nuclear lifetimes between Marathon-5S and Marathon-Ultra control rods is shown in Table 6-1. As shown, the Marathon-5S  $\frac{1}{4}$ -segment nuclear lifetime exceeds [[ ]] of the Marathon-Ultra nuclear lifetime.

As of the date of this report, a total of six (6) Marathon-5S control rods have been inserted in high duty locations at one domestic, and one international BWR. These six assemblies will be visually inspected after each two-year cycle. This exceeds the requirement in Section 3.3 of the Safety Evaluation in Reference 1 to visually inspect the two (2) lead use assemblies. For this surveillance program proposal, it is assumed that at least two of these Marathon-5S lead control rod assemblies will remain at a higher depletion than any Marathon-Ultra lead use assemblies until the Marathon-5S lead use assemblies have reached the end of their inspection campaign. In the unlikely event that lead Marathon-Ultra lead use assemblies pass the Marathon-5S lead use assemblies in terms of  $\frac{1}{4}$ -segment depletion, it is proposed that the Marathon-5S surveillance program described in Reference 1 be transferred to the Marathon-Ultra. Otherwise the following surveillance program is proposed.

- A minimum of two (2) Marathon-Ultra control rods will be inserted in high duty locations in a D, C, or S lattice, domestic or international BWR.
- Additional Marathon-Ultra control rods may be inserted in other domestic BWRs, with the intent that they remain at a lower depletion than the two lead depletion Marathon-Ultra control rods at the designated BWR. Should other control rods at a domestic or international BWR become the highest depletion in the BWR fleet, they will become the control rods inspected per this surveillance program.
- The two lead depletion control rods will be irradiated, achieving as close to nuclear end-of-life as practical (target minimum 90% of end-of-life).

NEDO-33284 Supplement 1 Revision 0  
Non-Proprietary Information

- For refueling outages in which the depletion of the lead Marathon-Ultra assemblies are greater than 75% of design nuclear life, the two (2) highest depletion Marathon-Ultra control rods will be moved to the spent fuel pool, with a visual inspection of all eight faces of each control rod performed. Lead Marathon-Ultra control rods may exceed 75% depletion prior to the eight-face inspections planned in the spent fuel pool as long as those inspections are performed before the control rods are utilized in another fuel cycle.
- For Marathon-Ultra control rods inserted in the opposite lattice type as the lead depletion units, two (2) highest depletion control rods shall be visually inspected during refueling outages in which the depletion of the control rods exceeds 90% of design nuclear life. These visual inspections shall consist of an inspection of all eight faces of the control rod. For the purpose of this surveillance program, D and S lattice applications are considered equivalent, since the geometry of the absorber tube and capsule are identical. For example, if the lead depletion control rods are in a D or S lattice plant, inspections of the lead C lattice Marathon-Ultra control rods shall be performed during outages for which the depletion exceeds 90% of the design nuclear life. Conversely, if the lead depletion Marathon-Ultra control rods are in a C lattice plant, additional inspections of D or S lattice Marathon-5S control rods shall be performed during outages for which the depletion exceeds 90% of the design nuclear life.
- To confirm the end-of-life performance of the Marathon-Ultra control rod, the first twelve (12) control rods of each lattice type (D/S lattice and C lattice) shall be visually inspected upon discharge, for a total of 24 visual inspections, not to exceed four (4) control rods from any single plant. These visual inspections shall consist of an inspection of all eight faces of the control rod.
- Should a material integrity issue be observed, GEH will (1) arrange for additional inspections to determine a root cause and (2) if appropriate, recommend a revised lifetime limit to the NRC based on the inspections and other applicable information available.
- GEH will report to NRC the results of all Marathon-Ultra visual inspections at least annually.

**Table 6-1**  
**Marathon-5S / Marathon-Ultra Nuclear Lifetime Comparison**

| <b>Application</b> | <b>End of Life B-10 <math>\frac{1}{4}</math>-Segment Equivalent Depletion (%)</b> |                       | <b>Ratio:<br/>Marathon-5S /<br/>Marathon-Ultra</b> |
|--------------------|---|-----------------------|--|
|                    | <b>Marathon-5S</b>  | <b>Marathon-Ultra</b> |  |
| D Lattice, BWR/2-4 | [[  |                       |  |
| C Lattice, BWR/4,5 |   |                       |  |
| S Lattice, BWR/6   |   |                       | ]]   |

## 7. EFFECT ON STANDARD PLANT TECHNICAL SPECIFICATIONS

The purpose and function of control rods are discussed in the Bases sections of the BWR/4 and BWR/6 Standard Technical Specifications (STS), References 4 and 5. Section B3.1.3, of both states:

*“...the CRD System provides the means for the reliable control of reactivity changes to ensure under conditions of normal operation, including anticipated operational occurrences, that specified fuel design limits are not exceeded. In addition, the control rods provide the capability to hold the reactor core subcritical under all conditions and to limit the potential amount and rate of reactivity increase caused by a malfunction in the CRD System.”*

The nuclear worth characteristics of the Marathon-Ultra CRB are compatible with the core cold shutdown requirements and hot operational requirements of the original equipment control rods. This is achieved by meeting the matched worth criteria, described in the Marathon LTR (Reference 1), as a reactivity worth within  $\pm 5\%$   $\Delta k/k$  of the reactivity worth of the original equipment CRB. Therefore, the Marathon-Ultra CRB provides the means for the reliable control of reactivity changes to ensure that under conditions of normal operation, including AOOs, specified fuel design limits are not exceeded. Furthermore, the Marathon-Ultra CRB provides the capability to hold the reactor core subcritical under all conditions, while meeting current Technical Specification shutdown margin requirements. The overall Marathon-Ultra assembly weight and velocity limiter design will limit the amount and rate of reactivity increase caused by a malfunction of the CRD system, i.e.) a Control Rod Drop Accident (CRDA).

Therefore, there is no effect on the STS from introduction of the Marathon-Ultra control rod blade.

## **8. PLANT OPERATIONAL CHANGES**

The fit, form and function of the Marathon-Ultra CRB are equivalent to the existing Duralife, Marathon, and Marathon-5S CRB designs. The Marathon-Ultra CRB meets all scram insertion criteria, reactivity control criteria, and CRDA.

No changes to the STS or their Bases (References 4 and 5) are needed. Therefore, it is expected that no plant-specific Technical Specifications (TS) or their Bases will require a change to implement the Marathon-Ultra control rod. Thus, no plant operating procedure change is expected, except for CRB replacement schedules. Therefore, the introduction of the Marathon-Ultra CRB has no effect on plant operations.

## **9. EFFECTS ON SAFETY ANALYSES AND DESIGN BASIS ANALYSIS MODELS**

### **9.1 ANTICIPATED OPERATIONAL OCCURRENCES AND OTHER MALFUNCTIONS**

As previously discussed, the reactivity worth of the Marathon-Ultra CRB is an equivalent replacement for previous control rod designs. Furthermore, the Marathon-Ultra CRB meets all scram time criteria. Therefore, use of the Marathon-Ultra CRB does not adversely affect the mitigating response function (i.e., scram) for AOOs.

Introduction of the Marathon-Ultra CRB is unrelated to the initiating events of the analyzed AOOs, and thus, the probabilities of the different AOOs occurring are unaffected.

Because the Marathon-Ultra CRB meets the existing design and licensing requirements for Marathon CRBs, the probability of any CRB-related malfunction or of causing a malfunction is not increased, and no new malfunction scenario is created.

The introduction of the Marathon-Ultra CRB does not (1) introduce a new failure mode or sequence of events that could result in the MCPWR safety limit being challenged, (2) cause a 10 CFR 50.2 design bases criterion or limit to be changed or exceeded (such that a safety-related function is adversely affected), (3) create a possibility of a new safety-related component interaction. Therefore, the change does not create a possibility for a malfunction of equipment important to safety different than previously evaluated.

In the safety analyses, the equipment modeled or assumed to function for mitigating the radiological consequences of all design basis abnormal events is not affected by the use of Marathon-Ultra CRBs. Therefore, the analyzed consequences of the malfunctions in plant Safety Analysis Reports are not affected.

### **9.2 ACCIDENTS**

The ECCS-LOCA performance, LOCA radiological, containment performance, and Main Steamline Break Accident (MSLBA) analyses all assume reactor scram within Technical Specifications requirements, and these are met by Marathon-Ultra CRBs. The Engineered Safety Feature (ESF) functions, which are modeled/assumed in the accident radiological consequence analyses, are also not affected by the use of Marathon-Ultra CRBs. Therefore, these analyses' models, scenarios, and the final radiological consequences are not affected.

The failures assumed in the initiating events for the LOCA and MSLBA are not related to the CRBs, and thus, the probabilities of these accidents occurring are not affected.

Other than the event evaluation assumption that the CRBs maintain structural integrity, the Fuel Handling Accident (FHA) initiating event and its related mitigation functions do not involve the CRBs. Therefore, the probability and consequences of a FHA are unaffected.

There is no additional friction between the Marathon-Ultra CRB relative to the Marathon CRB, and the CRD coupling mechanism is unchanged. Therefore, the probability of a stuck and

decoupled control rod occurring does not change, and thus, the probability of a CRDA cannot significantly increase.

The reactivity insertion rate during a CRDA is controlled by the weight of the control rod and by the shape of the velocity limiter. The Marathon-Ultra CRB remains within all rod drop parameters assumed or modeled in the safety analysis. Therefore, the analysis and consequences of a CRDA are unchanged.

The change to Marathon-Ultra CRBs does not create a new fission product release path, result in a new fission product barrier failure mode, or create a new sequence of events that results in significant fuel cladding failures. Therefore, the use of Marathon-Ultra CRBs cannot create an accident of a different type.

### **9.3 SPECIAL EVENTS**

The ATWS event assumes a failure to scram (without a specific cause) and that the Standby Liquid Control System is used for reactor shutdown. Therefore, the ATWS analysis scenario and results are independent of control rod blade design, and thus, the ATWS analysis is unaffected.

The station blackout, shutdown from outside control room, and safe shutdown fire analyses all assume reactor scram within TS requirements, which are not affected by the use of Marathon-Ultra CRBs. The other safe shutdown functions, which are modeled/assumed in the analyses, are also not related to or affected by the use of Marathon-Ultra CRBs. Therefore, these analyses' models, scenarios, and the final results are not affected.

### **9.4 FISSION PRODUCT BARRIER DESIGN BASIS LIMITS**

During all design basis events, Marathon-Ultra CRB performance is equal to or better than existing CRBs. The margins to the thermal limits on fuel cladding, Minimum Critical Power Ration (MCPR) Safety Limit, Reactor Coolant Pressure Boundary stress limits (e.g., temperature and pressure), and containment structural stress limits are unaffected by the use of Marathon-Ultra CRBs. Therefore, the fission product barrier design basis limits are not affected.

### **9.5 SAFETY AND DESIGN BASIS ANALYSIS MODELS**

Marathon-Ultra CRB implementation does not change any safety analysis input, model, or result. No design analysis methodology change is used or needed in the design of the Marathon-Ultra CRB. Therefore, this change does not involve a departure from a method of evaluation used in establishing a design basis or in a safety analysis

## 10. ABSORBER LOADING OPTIONS

In the future, GEH may offer alternate load patterns of boron carbide capsules and hafnium rods, within the Marathon-5S / Marathon-Ultra outer structure. For example, GEH may pursue an all-boron carbide capsule design, employing the Marathon-Ultra capsule. Also, the number and location of boron carbide capsules and hafnium rods may be varied to produce control rods of varying nuclear lifetime. Before any alternate load patterns are offered, a technical safety evaluation shall demonstrate that the control rods employing the alternate load patterns meet all the safety, design, and operational acceptance criteria presented within this report. This includes, but is not limited to:

- Demonstration of clearance between the boron carbide capsule and outer absorber tube at 100% local depletion, using  $+3\sigma$  boron carbide swelling and worst-case dimensions (Section 3.6.2).
- Demonstration of clearance between the hafnium rod and the outer absorber tube at end-of-life (Section 3.6.5).
- Demonstration of acceptable stresses due to control rod scram, against acceptance criteria (Section 3.3).
- Demonstration of conformance to nuclear evaluation design criteria in Section 4.1, using methodology equivalent to that in Section 4.2.

## 11. ABWR AND ESBWR DESIGNS

The BWR/2-6 Marathon-5S and Marathon-Ultra designs may also be adapted to ABWR and ESBWR applications. Both ABWR and ESBWR applications will use D/S lattice sized absorber tubes, boron carbide capsules, and hafnium rods. The primary difference in the control rod designs is the replacement of the velocity limiter with a connector for both ABWR and ESBWR, and a shorter absorber section for ESBWR. The connector is discussed in Section 2.4 of Reference 12. For ESBWR, the absorber section is approximately 9.5 feet versus approximately 12 feet for other BWR types. It is noted that despite these differences, the design methodologies between the BWR types are identical.

Before Marathon-5S or Marathon-Ultra control rods for ABWR and ESBWR are offered, a technical safety evaluation shall demonstrate that the control rods meet all the safety, design, and operational acceptance criteria presented within this report. This includes, but is not limited to:

- Demonstration of clearance between the boron carbide capsule and outer absorber tube at 100% local depletion, using  $+3\sigma$  boron carbide swelling and worst-case dimensions (Section 3.6.2).
- Demonstration of clearance between the hafnium rod and the outer absorber tube at end-of-life (Section 3.6.5).
- Demonstration of acceptable stresses due to control rod scram, against acceptance criteria (Section 3.3).
- Demonstration of conformance to nuclear evaluation design criteria in Section 4.1, using methodology equivalent to that in Section 4.2.

## **12. SUMMARY AND CONCLUSIONS**

The Marathon-Ultra control rod blade is designed as an acceptable direct replacement control rod for BWR/2-6. Conservative mechanical evaluations show acceptability of the control rod structure. Conservative nuclear analyses show that the Marathon-Ultra is a 'matched worth' control rod and is interchangeable with the original equipment.

Operational evaluations show no adverse effect on plant operations, including control rod scram, 'no settle' characteristics, and control rod drop.

The Marathon-Ultra control rod, which is a derivative of the Marathon design, meets all licensing acceptance criteria of the Marathon and Marathon-5S designs (References 1 and 2).

The introduction of the Marathon-Ultra CRB does not affect the Standard Technical Specifications (References 4 and 5) or their Bases, any plant safety analysis, or any plant design basis. In addition, no adverse effect is found when examining safety analyses and design basis analysis models. The Marathon-Ultra CRB meets all applicable design and regulatory requirements. Therefore, the use of the Marathon-Ultra CRB is judged to be acceptable.

### 13. REFERENCES

1. GE Hitachi Nuclear Energy, "Marathon-5S Control Rod Assembly," NEDE-33284P-A Revision 2, October 2009 and NEDO-33284-A, Revision 2, October 2009.
2. GE Nuclear Energy, "GE Marathon Control Rod Assembly," NEDE-31758P-A, October 1991 and NEDO-31758-A, October 1991.
3. MNCP4A – A General Monte Carlo N-Particle Radiation Transport Code, Version 4A, March 1994.
4. USNRC, "Standard Technical Specifications General Electric Plants, BWR/4," NUREG-1433 Vol. 1 & 2, Revision 3.0, June 2004.
5. USNRC, "Standard Technical Specifications General Electric Plants, BWR/6," NUREG-1434 Vol. 1 & 2, Revision 3.0, June 2004.
6. 1989 ASME Section III, Division 1, Appendix I, Figure I-9.2.1.
7. JA Bannantine, JJ Comer and JL Handrock, 'Fundamentals of Metal Fatigue Analysis', Prentice Hall, 1990.
8. BWRVIP-99, "Boiling Water Reactor Vessel and Internal Project: Crack Growth Rates in Irradiated Stainless Steels in BWR Internal Components," EPRI TR 1003018 Final Report, December 2001.
9. USNRC Information Notice 89-31, "Swelling and Cracking of Hafnium Control Rods," March 1989.
10. GE Hitachi Nuclear Energy, "GEH Marathon Control Rod Lifetime Surveillance Update," GENE-0000-0071-8269-R1-P, April 2009 and GENE-0000-0071-8269-R1-NP, April 2009.
11. GE Hitachi Nuclear Energy, "Marathon Control Rod Post-Irradiation Examination (PIE)," GENE-0000-0095-4020-R1-P, April 2009 and GENE-0000-0095-4020-R1-NP, April 2009.
12. GE Hitachi Nuclear Energy, "ESBWR Marathon Control Rod Mechanical Design Report," NEDE-33244P Revision 1, November 2007.

## APPENDIX A – FAILED BUFFER SCRAM STRESS EVALUATION

Failed buffer scram stress calculations for all cross-sections shown in Figures 3-1 and 3-2 are shown in Table 3-5 through 3-7. During a control rod scram, large axial loads are imparted on the control rod. These axial loads are determined using a dynamic spring and mass model, the results of which are presented in Table 3-4. For this analysis, the scram loads are determined assuming a 100% inoperative control rod drive buffer. The following cross-sections are analyzed.

### A-1 SOCKET MINIMUM CROSS-SECTIONAL AREA (FIGURE 3-1)

The minimum cross-sectional area of the socket is calculated from the drawing to be [[

]] Actual and allowable stress calculations are shown in Table A-1. As shown, all design ratios are less than 1.0. Therefore, the structure is acceptable.

### A-2 VELOCITY LIMITER TRANSITION SOCKET TO FIN WELD (FIGURE 3-1)

The transition piece to fin welds are double fillet welds, joining the type 316 transition piece and fins, with ER 308L filler metal required.

For the calculation of the area of these welds, only the vertical portions of the welds are considered. The angled portions of the welds are conservatively neglected (Figure 3-1). Also, since the welds are in shear, the resulting area is multiplied by  $(1/\sqrt{3})$  to calculate an equivalent normal area. The minimum equivalent normal weld area is calculated to be [[ ]]

Table A-2 shows the actual and allowable stresses for this weld. As shown, all design ratios are less than 1.0. Therefore, the weld is acceptable.

### A-3 VELOCITY LIMITER FIN MINIMUM CROSS-SECTIONAL AREA (FIGURE 3-1)

The minimum cross-sectional area of the fins is calculated from the drawing to be [[

]] Actual and allowable stress calculations are shown in Table A-3. As shown, all design ratios are less than 1.0. Therefore, the structure is acceptable.

### A-4 VELOCITY LIMITER TO ABSORBER SECTION WELD (FIGURE 3-2)

The weld connecting the absorber section to the velocity limiter is analyzed using the combined loading of the scram loads and axial loads due to the maximum allowable internal pressure of the absorber tubes.

Since both the scram loads and the load due to the internal pressure of the absorber tubes is considered, a combined weld area of the absorber section to handle weld, and the end plug to absorber tube weld is calculated. Since the end plug weld is in shear for this loading, the weld area is multiplied by  $(1/\sqrt{3})$  to calculate an effective normal weld area. This is added to the minimum absorber section to velocity limiter weld area, which is determined using CAD software:

$$A_{\text{normal}} = (\# \text{ Pressurized Tubes})(1/\sqrt{3})(\pi)OD_{\text{plug,min}}(\text{weld penetration}) \\ + (\# \text{ Tubes})(\text{absorber section to handle/VL area per tube}).$$

The weld area per tube is then multiplied by the number of tubes. The weld area calculation is summarized in Table A-4.

Once the effective normal weld area is known, the combined maximum stresses due to scram and internal pressure are calculated as described in Table A-5. As shown, all design ratios are less than 1.0. Therefore, the weld is acceptable.

#### **A-5 ABSORBER SECTION (FIGURE 3-2)**

The minimum cross-sectional area of the absorber section is calculated in Table A-6. Actual and allowable stresses are shown in Table A-7. As shown, all design ratios are less than 1.0. Therefore, the structure is acceptable.

#### **A-6 ABSORBER SECTION TO HANDLE WELD (FIGURE 3-2)**

The weld connecting the absorber section to the handle is analyzed using the combined loading of the scram loads and axial loads due to the maximum allowable internal pressure of the absorber tubes.

Since both the scram loads and the load due to the internal pressure of the absorber tubes is considered, a combined weld area of the absorber section to handle weld, and the end plug to absorber tube weld is calculated. Since the end plug weld is in shear for this loading, the weld area is multiplied by  $(1/\sqrt{3})$  to calculate an effective normal weld area. This is added to the minimum absorber section to handle weld area, which is determined using CAD software:

$$A_{\text{normal}} = (\# \text{ Pressurized Tubes})(1/\sqrt{3})(\pi)OD_{\text{plug,min}}(\text{weld penetration}) \\ + (\# \text{ Tubes})(\text{absorber section to handle/VL area per tube}).$$

The weld area per tube is then multiplied by the number of tubes. The weld area calculation is summarized in Table A-8. Once the effective normal weld area is known, the combined maximum stresses due to scram and internal pressure are calculated as described in Table A-9. As shown, all design ratios are less than 1.0. Therefore, the structure is acceptable.

#### **A-7 HANDLE MINIMUM CROSS-SECTIONAL AREA (FIGURE 3-2)**

The minimum cross-sectional areas of the handle, and actual and allowable stresses, are shown in the Table A-10. As shown, all design ratios are less than 1.0. Therefore, the structure is acceptable.

NEDO-33284 Supplement 1 Revision 0  
Non-Proprietary Information

**Table A-1 Socket Axial Stress Calculations**

| Description                          | Source                   | D Lattice |        | C Lattice |        | S Lattice |        |
|--------------------------------------|--------------------------|-----------|--------|-----------|--------|-----------|--------|
|                                      |                          | 70 °F     | 550 °F | 70 °F     | 550 °F | 70 °F     | 550 °F |
| Max Failed Buffer Scram Load (kips)  | Table 3-4                | [[        |        |           |        |           |        |
| Max Failed Buffer Scram Stress (ksi) | =P/1.919 in <sup>2</sup> |           |        |           |        |           |        |
| Allowable Stress (ksi)               | Table 3-2 (XM-19)        |           |        |           |        |           |        |
| <b>Design Ratio</b>                  | =stress/allow            |           |        |           |        |           | ]]     |

**Table A-2 Transition Socket to Fin Weld Stress Calculations**

| Description                          | Source              | D Lattice |        | C Lattice |        | S Lattice |        |
|--------------------------------------|---------------------|-----------|--------|-----------|--------|-----------|--------|
|                                      |                     | 70 °F     | 550 °F | 70 °F     | 550 °F | 70 °F     | 550 °F |
| Max Failed Buffer Scram Load (kips)  | Table 3-4           | [[        |        |           |        |           |        |
| Max Failed Buffer Scram Stress (ksi) | =P/A                |           |        |           |        |           |        |
| Allowable Stress (ksi)               | Table 3-2 (ER 308L) |           |        |           |        |           |        |
| Weld Quality Factor                  | Table 3-3           |           |        |           |        |           |        |
| Allowable Weld Stress (ksi)          | =S <sub>m</sub> *q  |           |        |           |        |           |        |
| <b>Design Ratio</b>                  | =stress/Allow       |           |        |           |        |           | ]]     |

NEDO-33284 Supplement 1 Revision 0  
Non-Proprietary Information

**Table A-3 Minimum Fin Area Stress Calculations**

| Description                          | Source                   | D Lattice |        | C Lattice |        | S Lattice |        |
|--------------------------------------|--------------------------|-----------|--------|-----------|--------|-----------|--------|
|                                      |                          | 70 °F     | 550 °F | 70 °F     | 550 °F | 70 °F     | 550 °F |
| Max Failed Buffer Scram Load (kips)  | Table 3-4                | [[        |        |           |        |           |        |
| Max Failed Buffer Scram Stress (ksi) | =P/A                     |           |        |           |        |           |        |
| Allowable Stress (ksi)               | Table 3-2<br>(316 plate) |           |        |           |        |           |        |
| <b>Design Ratio</b>                  | =stress/allow            |           |        |           |        |           | ]]     |

**Table A-4 Velocity Limiter to Absorber Section Weld Geometry**

| Description                                       | Reference               | D Lattice | C Lattice | S Lattice |
|---|-------------------------|-----------|-----------|-----------|
| Absorber Tube to VL Weld Area (in <sup>2</sup> )  | CAD analysis            | [[        |           |           |
| Min End Plug OD (in)                              | Drawing                 |           |           |           |
| Max End Plug OD (in)                              | Drawing                 |           |           |           |
| Min End Plug Weld Penetration (in)                | Assembly Drawing        |           |           |           |
| Number of Absorber Tubes per Assembly             | Assembly Drawing        |           |           |           |
| Number of Pressurized Absorber Tubes per Assembly | Assembly Drawing        |           |           |           |
| Total Weld Area (in <sup>2</sup> )                | Equation in Section A-4 |           |           | ]]        |

NEDO-33284 Supplement 1 Revision 0  
Non-Proprietary Information

**Table A-5 Velocity Limiter to Absorber Section Weld Stress Calculations**

| Description  | Source                                | D Lattice |        | C Lattice |        | S Lattice |        |
|--|---------------------------------------|-----------|--------|-----------|--------|-----------|--------|
|  |                                       | 70 °F     | 550 °F | 70 °F     | 550 °F | 70 °F     | 550 °F |
| Max Failed Buffer Scram Load (kips)                      | Table 3-4                             | [[        |        |           |        |           |        |
| Maximum Allowable Internal Pressure (ksi)                | Finite Element Analysis               |           |        |           |        |           |        |
| End Plug Pressure Area (in <sup>2</sup> )                | = $\pi/4*(OD_{plug})^2$               |           |        |           |        |           |        |
| Number of Pressurized Tubes                              | Assembly Drawing                      |           |        |           |        |           |        |
| Total Axial Load (kips)                                  | =Scram Load + (press)(area) (# tubes) |           |        |           |        |           |        |
| Total Weld Area (in <sup>2</sup> )                       | Table A-4                             |           |        |           |        |           |        |
| Max Failed Buffer Scram + Internal Pressure Stress (ksi) | = $P_{tot}/A$                         |           |        |           |        |           |        |
| Allowable Stress (ksi)                                   | Table 3-2 (304S Tubes)                |           |        |           |        |           |        |
| Weld Quality Factor                                      | Table 3-3                             |           |        |           |        |           |        |
| Allowable Weld Stress (ksi)                              | = $S_m*q$                             |           |        |           |        |           |        |
| <b>Design Ratio</b>                                      | =Stress/Allow                         |           |        |           |        |           | ]]     |

**Table A-6 Absorber Section Geometry Calculation**

| Description  | Source                               | D Lattice | C Lattice | S Lattice |
|--|--------------------------------------|-----------|-----------|-----------|
| Min Absorber Tube Area (in <sup>2</sup> )                              | CAD Analysis                         | [[        |           |           |
| Min Tie Rod Area (in <sup>2</sup> )                                    | CAD Analysis                         |           |           |           |
| Number of Absorber Tubes   | Assembly Drawing                     |           |           |           |
| Total Minimum Absorber Section Cross-sectional Area (in <sup>2</sup> ) | =(# tubes)(tube area) + tie rod area |           |           | ]]        |

NEDO-33284 Supplement 1 Revision 0  
Non-Proprietary Information

**Table A-7 Absorber Section Stress Calculation**

| Description                          | Source                 | D Lattice |        | C Lattice |        | S Lattice |        |
|--------------------------------------|------------------------|-----------|--------|-----------|--------|-----------|--------|
|                                      |                        | 70 °F     | 550 °F | 70 °F     | 550 °F | 70 °F     | 550 °F |
| Max Failed Buffer Scram Load (kips)  | Table 3-4              | [[        |        |           |        |           |        |
| Max Failed Buffer Scram Stress (ksi) | =P/A                   |           |        |           |        |           |        |
| Allowable Stress (ksi)               | Table 3-2 (304S Tubes) |           |        |           |        |           |        |
| <b>Design Ratio</b>                  | =stress/allow          |           |        |           |        |           | ]]     |

**Table A-8 Absorber Section to Handle Weld Area Calculation**

| Description  | Source                | D Lattice | C Lattice | S Lattice |
|--|-----------------------|-----------|-----------|-----------|
| Absorber Tube to Handle Weld Area (in <sup>2</sup> ) | From CAD analysis     | [[        |           |           |
| Min End Plug OD (in)                                 | From drawing          |           |           |           |
| Max End Plug OD (in)                                 | From drawing          |           |           |           |
| Min End Plug Weld Penetration (in)                   | From assembly drawing |           |           |           |
| Number of Absorber Tubes per Assembly                | Assembly Drawing      |           |           |           |
| Number of Pressurized Absorber Tubes per Assembly    | Assembly Drawing      |           |           |           |
| Total Weld Area (in <sup>2</sup> )                   | =(# tubes)(area)      |           |           | ]]        |

NEDO-33284 Supplement 1 Revision 0  
Non-Proprietary Information

**Table A-9 Absorber Section to Handle Weld Stress Calculations**

| Description  | Source                                | D Lattice |        | C Lattice |        | S Lattice |        |
|--|---------------------------------------|-----------|--------|-----------|--------|-----------|--------|
|  |                                       | 70 °F     | 550 °F | 70 °F     | 550 °F | 70 °F     | 550 °F |
| Max Failed Buffer Scram Load (kips)                      | Table 3-4                             | [[        |        |           |        |           |        |
| Maximum Allowable Internal Pressure (ksi)                | Finite Element Analysis               |           |        |           |        |           |        |
| End Plug Pressure Area (in <sup>2</sup> )                | = $\pi/4*(OD_{plug})^2$               |           |        |           |        |           |        |
| Number of Pressurized Tubes                              | From assembly drawing                 |           |        |           |        |           |        |
| Total Axial Load (kips)                                  | =Scram Load + (press)(area) (# tubes) |           |        |           |        |           |        |
| Total Weld Area (in <sup>2</sup> )                       | Table A-8                             |           |        |           |        |           |        |
| Max Failed Buffer Scram + Internal Pressure Stress (ksi) | = $P_{tot}/A$                         |           |        |           |        |           |        |
| Allowable Stress (ksi)                                   | Table 3-2 (304S Tubes)                |           |        |           |        |           |        |
| Weld Quality Factor                                      | Table 3-3                             |           |        |           |        |           |        |
| Allowable Weld Stress (ksi)                              | = $S_m * q$                           |           |        |           |        |           |        |
| <b>Design Ratio</b>                                      | =Stress/Allow                         |           |        |           |        |           | ]]     |

**Table A-10 Handle Scram Stress Calculations**

| Description                          | Reference             | D Lattice |        | C Lattice |        | S Lattice |        |
|--------------------------------------|-----------------------|-----------|--------|-----------|--------|-----------|--------|
|                                      |                       | 70 °F     | 550 °F | 70 °F     | 550 °F | 70 °F     | 550 °F |
| Max Failed Buffer Scram Load (kips)  | Table 3-4             | [[        |        |           |        |           |        |
| Max Failed Buffer Scram Stress (ksi) | = $P/A$               |           |        |           |        |           |        |
| Allowable Stress (ksi)               | Table 3-2 (316 plate) |           |        |           |        |           |        |
| <b>Design Ratio</b>                  | =stress/allow         |           |        |           |        |           | ]]     |